COLLEGE OF NATURAL SCIENCES

SCHOOL OF EARTH SCIENCES

APPLICATION OF GRAVITY AND MAGNETIC METHODS TO CHARACTERIZE SUBSURFACE STRUCTURES CONTRIBUTING TO GROUND WATER FLOW IN THE MEKI-BULBULA RIFT CORRIDOR, CMER

A THESIS SUBMITTED TO

THE SCHOOL OF EARTH SCIENCES OF ADDIS ABABA UNIVERSITY IN PARTIAL FULFILLMENT OF THE REQUIREMENTS FOR THE DEGREE OF MASTER OF SCIENCE IN EXPLORATION GEOPHYSICS.

BY: TOLU WAKGARI

Addis Ababa University
Addis Ababa, Ethiopia

May 2018

ADDIS ABABA UNIVERSITY

COLLEGE OF NATURAL SCIENCE

SCHOOL OF EARTH SCIENCES

This is to certify that the thesis prepared by **Tolu Wakgari**, entitled: **"Application of Integrated geophysical methods to characterize subsurface structures contributing to groundwater flow in the Meki-Bulbula rift corridor, CMER"** and submitted in partial fulfillment of the requirements for the degree of Master of Science in Exploration Geophysics complies with the regulations of the university and meets the accepted standards with respect to originality and quality.

Approved by examining committee:

	Signature	Date
1. Dr. Balemwal Atnafu (Head, School of Earth Sciences)	_____	_____
2. Dr. Abera Alemu (Advisor)	_____	_____
3. Dr. Dessie Nedaw (Co - Advisor)	_____	_____
4. Prof. Tilahun Mammo (Examiner)	_____	_____
5. Dr. Ameha Atnafu (Examiner)	_____	_____

DECLARATION

I, the undersigned, hereby declare that this thesis is my original work carried out under the supervision of Dr. Abera Alemu and Dr. Dessie Nedaw and has not been presented as a thesis for a degree program in any other university and that all resources of materials used for the thesis are duly acknowledged.

Name: Tolu Wakgari

Signature: _____

Date: _____

This thesis has been submitted for examination for approval as university Advisor:

Name: Dr. Abera Alemu

Signature: _____

Date: _____

ACKNOWLEDGEMENT

Above all, I would like to express my heartfelt gratitude and appreciation to my Advisor,

Dr Abera Alemu**,** for that he sacrified his time to earn his scientific advice and guidance, constructive suggestions and all way round support from the beginning to the completion of this work. My gratefulness also goes to my Co-advisor, Dr. Dessie Nedaw for that he has been beside me by constructive advice.

I am grateful to the School of Earth Sciences of the Addis Ababa University and all staff of Geophysics and Institute of Geophysics, Space Science and Astronomy (IGSSA) for allowing me all facilities and advice to carry out my field and office work.

I would like to thank Hailemichael Kebede for his genuine support and guidance during office work. All members MSc Geophysics Graduate students are greatly acknowledged for their encouragement and genuine cooperation.

I gratefully acknowledge my mother for her moral assistance and encouragement above every one through so many complexities.

Table of contents

Contents

List of figures

ACRONYMS

2D	Two-dimensional
3D	Three-dimensional
AVC	Aluto Volcanic Complex
CMER	Central Main Ethiopian Rift
EC	Electrical Conductivity
ER	Ethiopian Rift
EARS	East African Rift System
FFT	Forward Fourier Transform
GPS	Geographic positioning system
GSE	Geological survey of Ethiopia
IGRF	International Geomagnetic Reference Field
IGSN	International Gravity Standardization Network
m asl	meter above sea level
MER	Main Ethiopian Rift
msl	Mean sea level
nT	Nano Tesla
NE	North East
NE –SW	North East – South West
N - E	North – East
NMER	Northern Main Ethiopian Rift
SI	Structural Index
SMER	Southern Main Ethiopian Rift
WFB	Wonji Fault Belt

ABSTRACT

The objective of this MSc thesis is to characterize subsurface structural influences on groundwater flow in the Meki-Bulbula rift Corridor located in the central main Ethiopian rift using integrated geophysical methods namely, gravity and magnetic methods.

The surface geology of the study area ranges in composition from volcanic rocks of rhyolite, pyroclastic, obsidian, and ignimbrite rocks, to lacustrine sediment and alluvial deposits. It is determined that the tectonic setting and rock types of an area are important in establishing the distribution of the groundwater flow.

Existence and orientation of subsurface linear structures, which may include faults, fractures, and veins have been investigated in the Meki-Bulbula rift Corridor using horizontal gradient gravity map and tilt derivative magnetic map compiled for the study area. These geophysical investigation results have identified subsurface geologic structures, which are responsible for the flow of groundwater from Meki to Bulbula. The depth, distribution and location of the subsurface geologic structures have been shown by Euler deconvolution gravity and magnetic maps.

Additionally, field observations made during the magnetic survey have confirmed the flow of ground water from Lake Ziway towards Lake Langano. This conclusion is also confirmed by the existence of hot springs at the northern shore of Lake Langano, which is missing at the southern shore of Lake Ziway.

This work has shown that there are no east west structures that favor the flow of groundwater.

Hence, the direction of groundwater flow in the study area takes place from Lake Ziway towards

Lake Langano being controlled by the N-S and NE-SW oriented faults and fractures mapped in the Meki – Bulbula corridor.

CHAPTER ONE

1 Introduction

1.1 Background

Geophysical surveys have long been utilized by the mining and petroleum industries for several decades and used to determine, indirectly, the extent and nature of the subsurface geologic materials. With further development, geophysical techniques have found applications in wider areas of earth sciences addressing engineering geology, hydrogeology and environmental issues, among others.

Potential field methods namely gravity and magnetic methods have been conducted to study the type of subsurface topography and geological structures like fault and fracture system of the area which are so much essential to characterize the basement of the basin.

A combination of gravity and magnetic surveys help to characterize large-scale (regional) basin structures. This integration of gravity and magnetic data reduces ambiguity by providing more rock characteristics that help to map structures and distinguish lithological units of a survey area.

Data processing and interpretation was made to characterize and better understand subsurface structures/geology of the basin for possible direction and relative magnitude (potential) of groundwater flow. Processing results in an anomalous field that is the reflection of subsurface topography, voids, faults and buried stream valleys.

This research work focuses on the identification of the subsurface geology controlling groundwater flow of the Meki-Bulbula and its adjacent basins. From this subsurface structure study, it is identified that there is subsurface hydraulic link within basin and inter-basin.

1.2 Location and accessibility of the study area

The study area is located about 180 km southeast of Addis Ababa, in the Central MER. The study area covers an area of approximately 3100 square km. Geographically the study area, Meki-Bulbula locality is bounded within the limit of $38^0$30'-$39^0$00' E Longitude (450000-510000 UTM) and $7^0$45'-$8^0$15' N Latitude (850000-910000 UTM) (Fig. 1.1).

The study area can be accessed through the asphalted road passing through Adami Tulu to the Aluto-Langano geothermal field to Lake Langano, passing through the Aluto geothermal base camp and it joins the asphalted road again at Bulbula and passing from Ogolcho, returning back to Meki through gravel road and passing from Meiki-Dugda-Koshe and returning back to asphalted road through Bulbula.

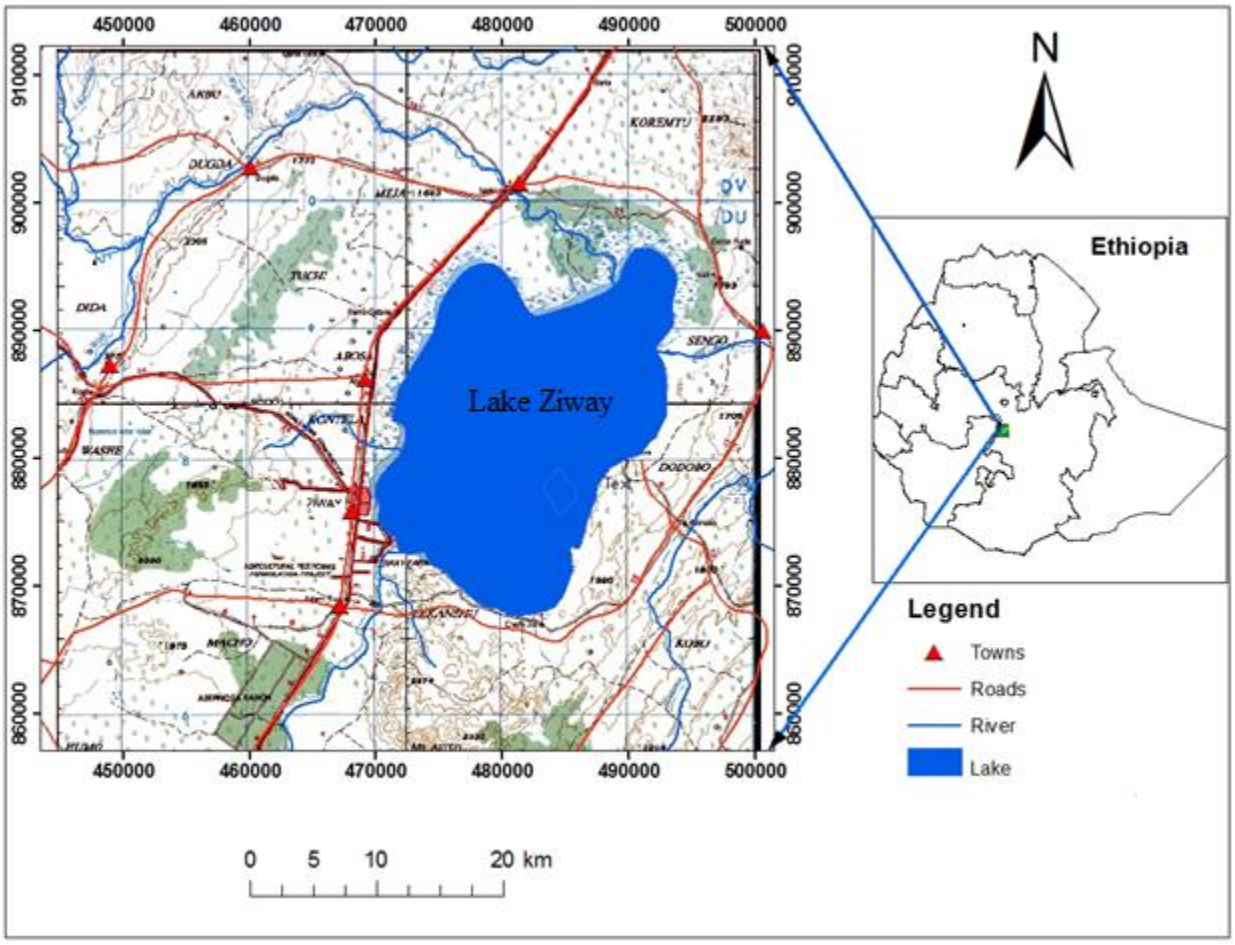

Fig. 1.1 Location map of the study area

1.3 Physiography

The topography of the Meki-Bulbula rift corridor dominantly lies at low altitude which varies from 1577 meter above sea level (m asl) to 1770 m asl. The western and eastern part of it is bounded by the rift escarpment (Fig.1.2).

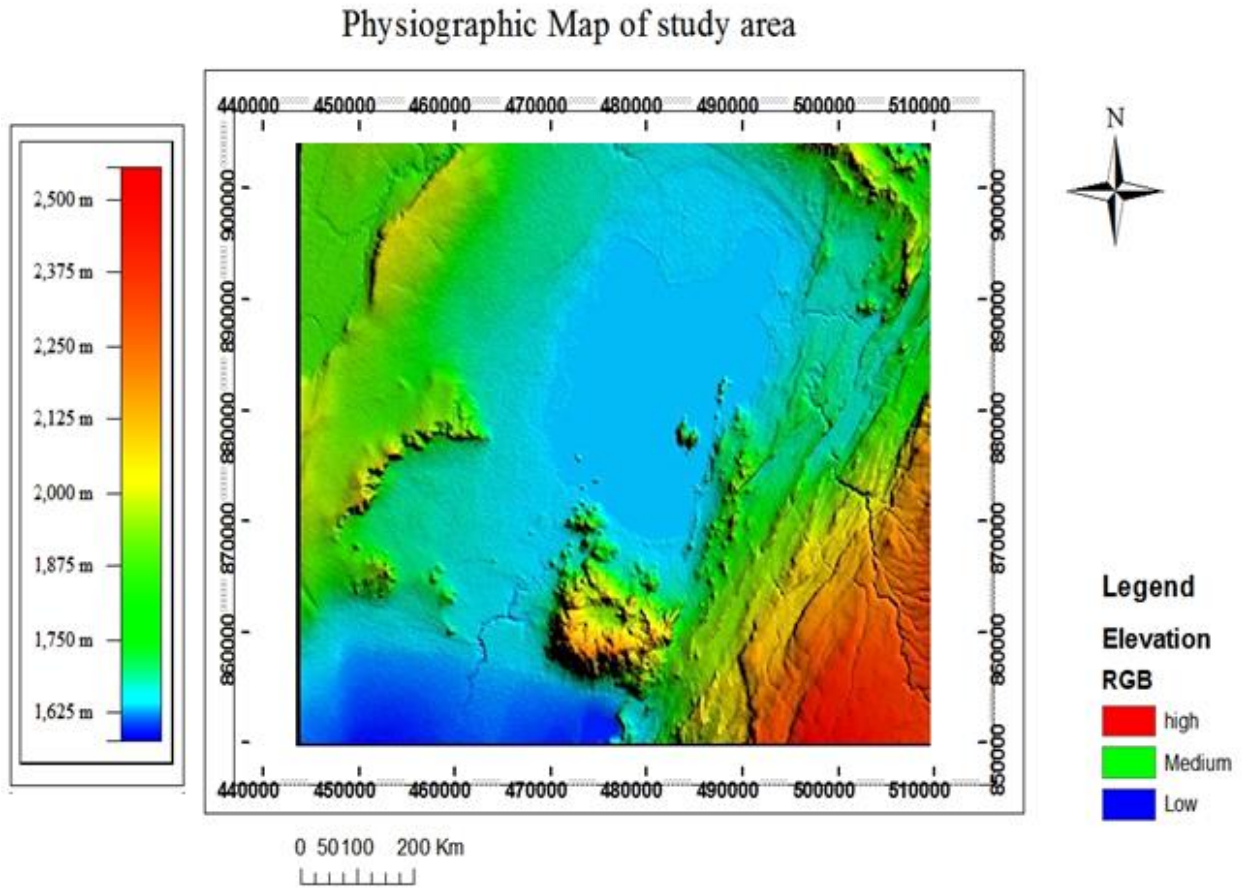

Fig. 1.2 Physiographic map of the study area

Existing mountains within the rift corridor are Aluto Volcano and Gademota caldera which are located on the southwestern and western part of the study area, respectively. Lowest elevations with in the area are Lake Ziway level (1637 m asl.), and gorges just like that of Abijata lake level (1577 m asl) and Meki Rivers.

Relative to the western margins the eastern and the southeastern rift margin of the study area; the central to the southern rift margin is marked by water bodies including Lake Ziway, deep gorges and canyons due to the existence of large regional marginal fault system.

Calderas observed in the study area are Aluto caldera located in the southern and Gademota Caldera south- western part of Lake Ziway.

1.4 Climate and vegetation cover

The Meki-Bulbula rift corridor appears to be a prominent topographic feature relative to the surrounding flat lands and the lake levels of Ziway (1685 m asl), Abijata (1577 m asl) and Langano

(1535 m asl). The study area is characterized by warm to cool, semi-humid zone, where the annual rainfall is more than 1000 mm and it is a semi-humid to arid zone (Mesfin Tadesse, 2017). Vegetation in the floor of the rift is dominated by the spiny acacia trees and some short bushes. The top of Aluto, in particular the obsidian flows and domes are covered by denser vegetation consisting of a variety of trees and bushes.

1.5 Drainage

Meki, Katar and Bulbula are the main and crucial rivers for scientific and economical purposes, which drain the study corridor.

Meki river is one of the feeding rivers to the lake Ziway on its north western part which raise from the Guraghe high lands. About 462 hectares of land is currently under cultivation using Meki River and its tributaries up stream of Meki town (Alemu D., 2006). Other than this, the river contributes large sand deposit and supply to different towns including Addis Ababa.

Katar River is another feeding river on the eastern part of the lake Ziway, which arise from the Arsi high lands. Bulbula River is an out let of Lake Ziway on the south western and as feeding river for Lake Abijata. Generally, tributary drainages are fine dendritic to sub-parallel. Patterns are controlled by topography and structures.

1.6 Previous geophysical, geological and hydrological works

Various geophysical, geological and hydro geological studies have been conducted in the study area, Meki-Bulbula vicinity that includes a portion of the Ziway-Shala basin. Volcanism, tectonics, and climate forcing were the responsible factors for the formation and sedimentation of this basin (Le Turdu et al., 1999). The complex relations among Late Quaternary deposits, landforms and soils have been mapped and described (Benvenuti et al., 2002). They updated the knowledge of Late Quaternary evolution of the area and attempted to correlate lake fluctuations, as proxies to climate change, with geomorphic evolution of non-lacustrine area.

Most of the gravity surveys are conducted in regional scale in the MER (Alemu, 1992) to investigate the crustal structure of the MER. There exists several gravity investigations on a semi-regional and local scale in the central MER that consists of the present study area (eg. Searl and Gouin, 1972; Alemu, 1983; Saibi, 2012).

Gravity and magnetic investigations have been made in the central MER on a semi-regional and local scale (Tsegay Berhane, 2015: Yemane Kelemework, 2016; Mesfin Tadesse, 2017) for geothermal and ground water exploration and investigating the crustal structure including the subsurface geological and structural conditions in the central MER.

1.7 Statement of the problem

Gravity and magnetic methods have been applied to map subsurface structures, contributing to ground water flow in the Meki-Bulbula rift corridor.

Numerical groundwater flow modeling (Tenalem Ayenew, 2001), isotopes hydrology and Geochemistry (Kebede et al., 2007) were used to identify the subsurface structures that may be determinants of the relative magnitude and direction of groundwater flow within the Ziway-Abijata sub-basin.

Based on the points mentioned above, this geophysical investigation is sought to know:

-Existence or non existence of subsurface geologic structures that act as conduits for groundwater flow

-Presence of subsurface hydraulic link between the Ziway-Langano and Ziway-Abijata Lakes

-The overall groundwater flow direction in the Meki-Bulbula rift corridor

1.8 Objective of the study

1.8.1 General objective

To map and characterize the groundwater flow along the Meki-Bulbula rift corridor using gravity and magnetic methods in order to identify subsurface structures contributing to groundwater flow.

1.8.2 Specific Objectives

- ✓ To integrate the gravity and magnetic data with the existing geological and other relevant data for further interpretations.
- ✓ To map the major structures and identify subsurface weak zones that serve as a storage areas or conduits for groundwater movement.
- ✓ Establish a relationship between the gravity and magnetic data with subsurface lineated geological structures and lithological units exposed on the surface.

- ✓ Map the locations, determine the orientations and estimate the possible depths of the major lineated geologic structures that control groundwater flow in the study area.

1.9 Significance of the present work

The significance of the present work could be enumerated as follows:

-It will provide a more recent and reliable gravity and magnetic data in this volcanically dynamic area, which can set a better basis for further investigations

-The result of the research work is also expected to provide an implication to geohazard impacts related to tectonics, volcanism and volcanic activities which in turn affect the ground water flow of the area under consideration

-The newly acquired magnetic data can contribute to the explorations of different kinds of natural resources, primarily for identifying promising areas of geothermal resources.

1.10 Methodology

The methodology involves three steps: Pre-field work, Fieldwork and post fieldwork.

1.10.1 Pre-field work

Before going to the study area for field data collection, preliminary works carried out include:

Literature review on the general geological and tectonic setting of the area under study

A review of geophysical studies carried out in the area and

Compilation of secondary data (gravity and magnetic data)

1.10.2 Field work

Having going through the office work (Pre-field work); a preparation for the actual field work to collect the necessary field data was conducted as per the procedures of the respective geophysical survey techniques. Accordingly, the required magnetic data is collected in the field.

1.10.2.1 Magnetic Survey

Ground based magnetic measurements have been made using Proton Precision magnetometer and hand held GPS apparatus.

The GPS data has been used to locate the position of the magnetic stations and to correct the magnetic data for the IGRF.

Magnetic data has been collected randomly and a base station is established. At each station, the magnetometer reading, recording time and the station location were recorded.

1.10.3 Post fieldwork

In this step, the collected data have been processed using different mapping software packages; including Arc GIS, Geosoft Oasismontaj, Global mapper, etc. and the results have been interpreted qualitatively and quantitatively. Finally, the research work has been compiled and presented as thesis.

Flow chart of the methodology

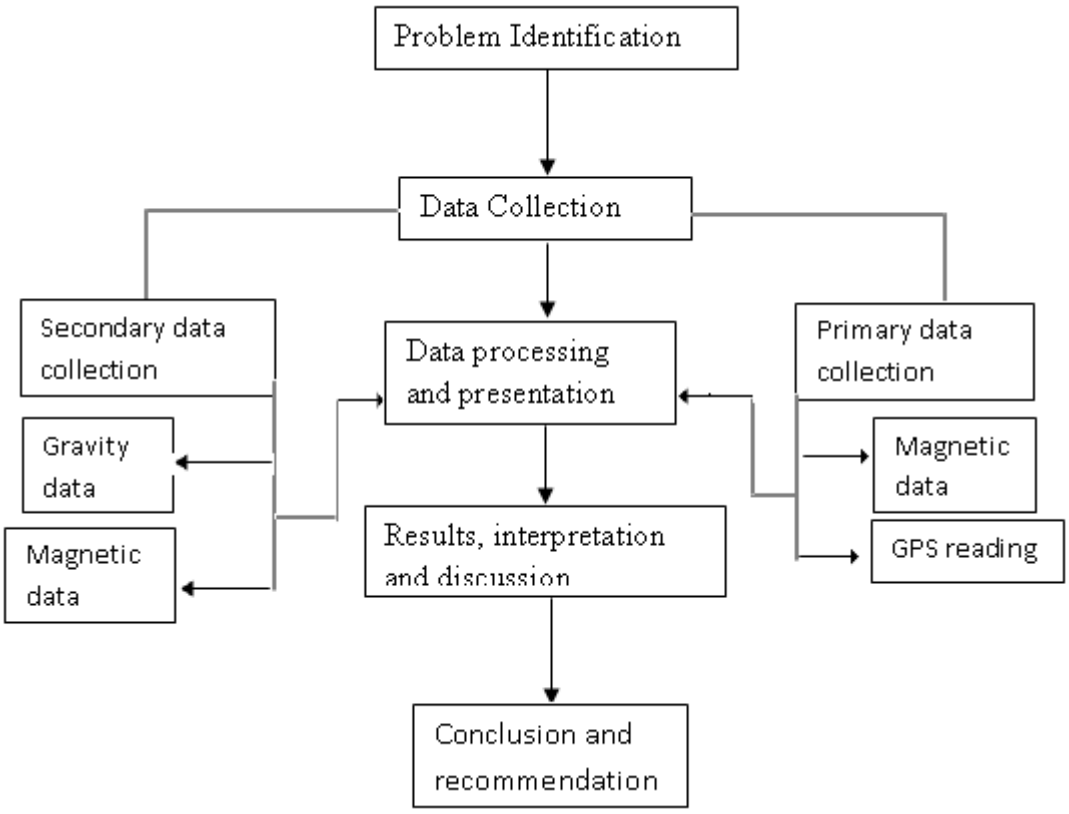

Fig. 1.3 Flow chart of methodology

1.10.4 Materials and software

Topographic map with a scale of 1:50,000 and geological maps of different scales have been used to know the surficial distribution of lithological and structural features of the study area. Google Earth map has been used to assess the overall setting of the study area before going to the field,

Proton precession magnetometer (MP-2) was used for magnetic data collection, Geographic positioning system (GPS) to record the exact data location points,

Arc GIS 10.3 for the preparation of location and base map and other GIS analysis,

Global mapper 12 and surfer 10 to post, extrapolate and analyze gravity and magnetic data

Geosoft oasis montaj is used for processing and presenting the compiled data

1.11 Structure of the thesis

This MSc thesis is organized into six chapters. Chapter one deals with the introduction part which includes background, location of the study area, physiography, statement of the problem, objective, methodology and materials, previous works, significance of the study. Chapter two consists regional geology and tectonics, geology of the study area with reference to EARS and MER. Chapter three deals with the theoretical background of the geophysical methods namely gravity and magnetic methods used in the present thesis work, which are collected from different sources. The background of the principles, instrumentations, data reduction processes and interpretations followed in both gravity and magnetic methods of prospecting are explained briefly in this chapter. Chapter four discusses about data acquisition, reduction, processing and presentation. In this chapter, the type of geophysical instruments used, data processing and data presentation schemes have been discussed. Chapter five is concerned about results, discussions and interpretations. The different maps generated and research results are discussed and interpreted briefly here. In chapter Six, Conclusions and Recommendations regarding the results of the work are outlined. Lastly, list of references in an alphabetical order is presented.

CHAPTER TWO

2 GEOLOGIC AND TECTONIC SETTING

2.1 Regional geology and tectonic setting

Several researchers (Corti,G., 2009; Boccaletti et al., 1999) have confirmed that the Ethiopian Rift (ER) system is part of the East African Rift System (EARS) and comprises a series of rift zones extending over a distance of about 1000 Km from the Afar Triple Junction at Red Sea – Gulf of Aden intersection to the Kenya Rift (KR) (Fig.2.1, Inset).

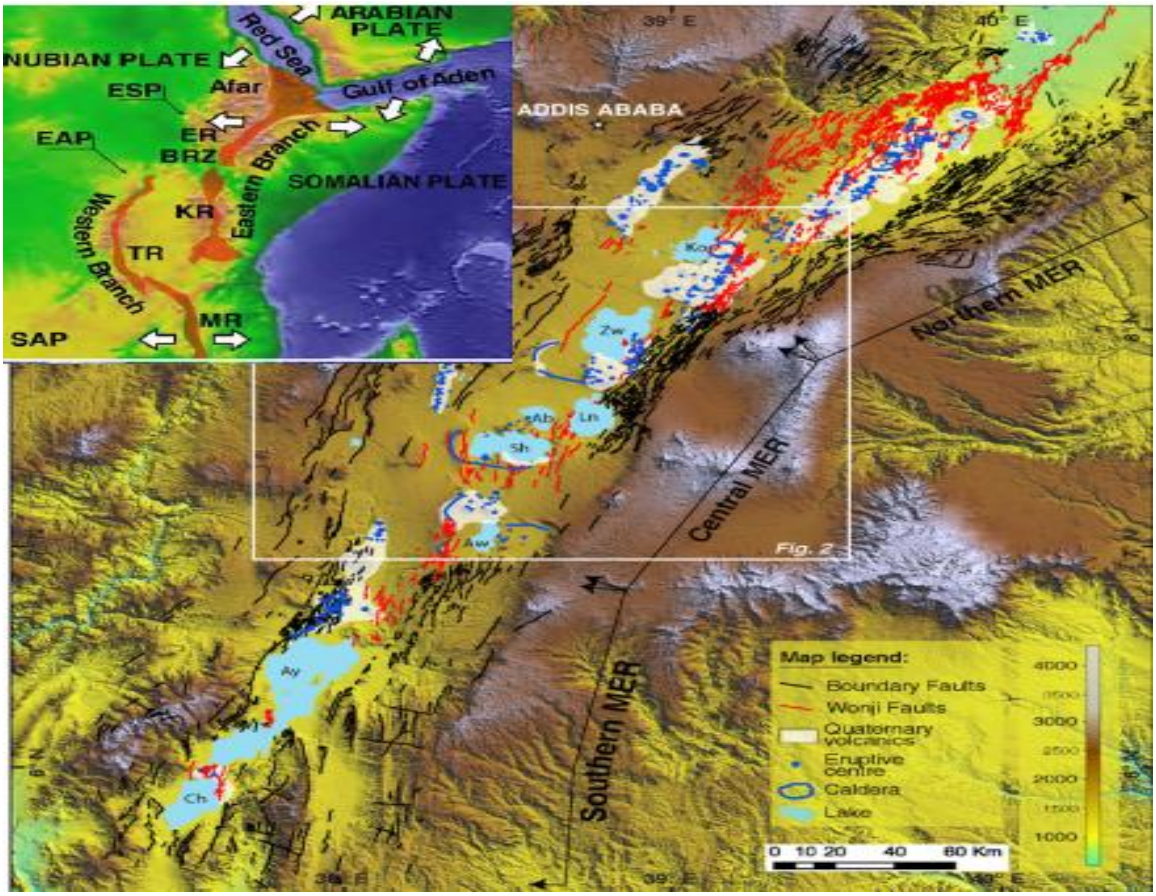

Fig. 2.1 Tectonic setting of the Main Ethiopian Rift (MER) in relation to the East African Rift System

Several workers (Davidson and Rex, 1980; Corti G., 2009) have shown that the Ethiopian Rift (ER) system is divided into three segments: the Afar Depression, the Main Ethiopian Rift (MER) and the ~300 km wide system of basins and ranges referred to as Broadly Rifted Zone (BRZ) (Fig. 2.1, Inset).

The MER divides the 1,000 km wide uplifted Ethiopian volcanic province asymmetrically into the northwest and southeast plateaus (Gidey et al., 1990). Volcanic sequences that cover an area several hundred kilometers across are more voluminous and widespread on the northwest plateau than on the southeastern plateaus. According to Gidey et al. (1990); Bonini et al. (2005); Corti (2009), the MER is geographically divided into three sectors: Northern MER (NMER), Central MER (CMER) and Southern MER (SMER) (Fig. 2.1).

The NMER is considered to extend from the Afar depression up to the Lake Koka region. The CMER encompasses most of the Lakes region up to the Lake Awasa area (Bonini et al., 2005). The SMER extends south of Lake Awasa into the Broadly Rifted Zone (BRZ) that characterizes the overlapping area between the Ethiopian and Kenya Rifts (Bonini et al., 2005).

These three segments of the MER represent different stages of extensional process, from early rifting in the SMER to more advanced stages in the CMER and NMER preceding the incipient seafloor spreading in Afar (Hayward and Ebinger, 1996). However, the age of onset of faulting and volcanism for the three segments of the MER point to a heterogeneous time-space evolution and progression of the continental rifting process along the MER.

The present study area is located in the tectonically active CMER which is bounded by the Yerer-Tulluwellel volcano tectonic lineament (YTVL) to the north and the Goba–Bonga tectonic lineament (GBTL) to the south (Fig. 2.2). In the study area, the CMER is bounded by the Munesa fault escarpment (major rift border) to the east and the Guraghe rift margin (major rift border) to the west (Fig. 2.2).

Four lakes namely Lake Ziway, Abiyata, Langano and shala which are believed to have been formed by volcano-tectonic processes occupy the CMER. As a result of differences in the geomorphologic setting they vary considerably in depth, shape, and size. The first three lakes have an elongated shape parallel to the main trend of the MER and can be defined as tectonically controlled lakes. Unlike the other three, Lake Shala occupies a caldera. The western part of the lake lies in a tectonically controlled depression. Thus, Lake Shala can be classified as volcano-tectonically controlled lake. The volcanic products of the whole Ethiopian Rift has been subdivided into six main tectono-magmatic chronozones since the Eocene – Oligocene and among these, the WFB-related volcanism represents the most recent volcano-tectonic activity in the MER (Wolde Gabriel et al., 1990).

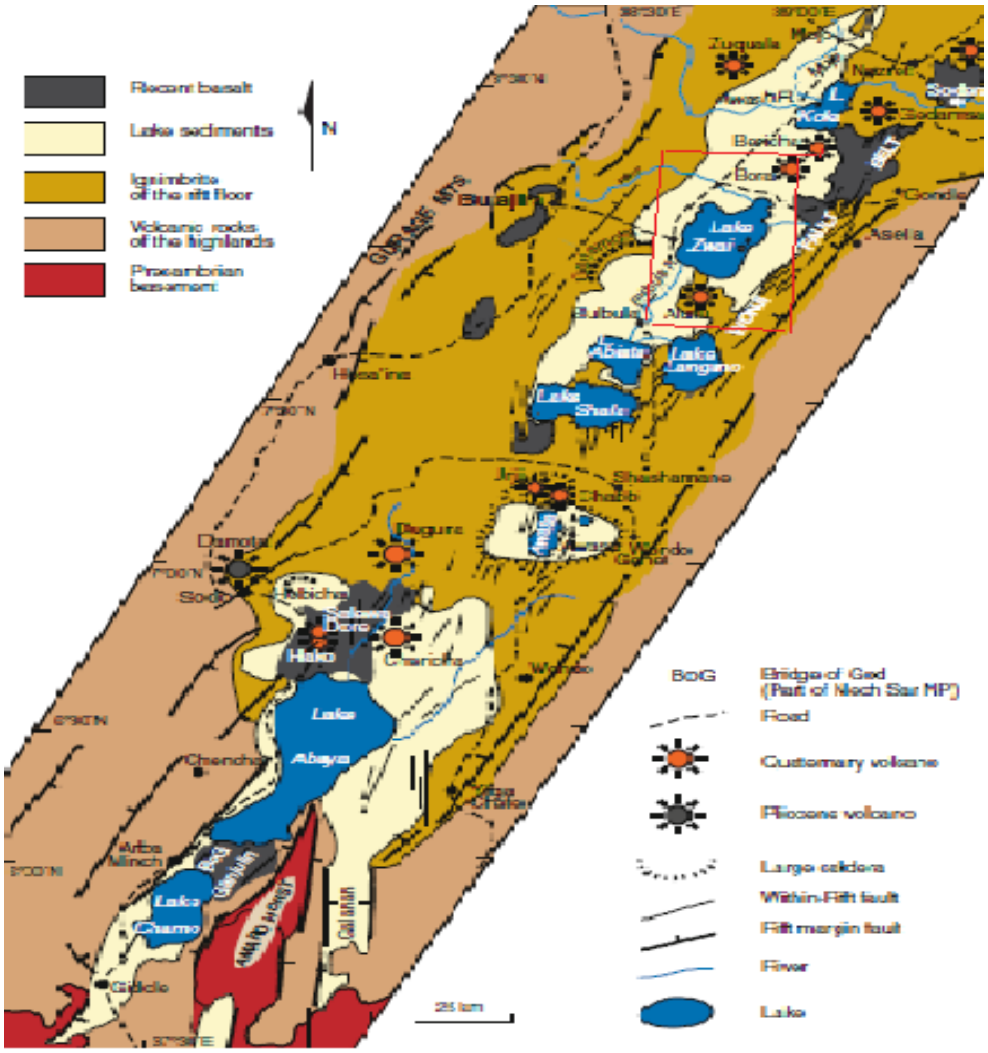

Fig. 2.2Geological map of the MER

(Modified from Saibi et al., 2012)

2.2 Geology and structural setting of the study area

Structural pattern of the study area is characterized by two main fault systems. These include a roughly 030º-040º trending border fault system and a 000º-020º trending fault system (WFB) mainly affecting the rift floor (Mohr, 1962), NE-SW trend of the MER, the WFB is characterized by active NNE-SSW trending extensions, fractures and normal faults.

In the study area the NW fracture system is visible cross-cutting the NE major faults system, forming small rhombic terrains in the south-eastern parts of the AVC, in particular between

Munesa and Aluto and to a minor extent in its south-central and northern parts. The south-central NW faults cross Aluto diagonally and connect several important hydrothermal manifestations

2.2.1 Structural setting of the study area

2.2.1.1 The ENE-WSW or Gulf of Aden Trend

Some volcanic centers on the rift margin and within the rift itself follow the ENE trend, but are not as important as the NW-SE trend. The Aluto caldera follows the same trend. Moreover, the southern rim of the caldera is made up of a chain of volcanic centers' and craters that are elongated and aligned in an E-W direction. It is clear that the southern part of the AVC is much higher than its northern part, probably due to the fact that a northward breaching took place at Aluto before the caldera collapse.

2.2.1.2 The NE-SW or Ethiopian Rift Trend

In the study area, the NE-SW trending faults and tectonic features are mainly expressed in the eastern and SE sectors and most of them deviate towards N, forming the NNE. Some of the volcanic centers, including the youngest three centers situated in the north-western part of the caldera, follow a NE-SW trend. This system has contributed significantly to the external and internal structural configuration of AVC. One of the important considerations refers to the fact that the older rock units, such as the [qw*Munesa crystal ignimbrite and the overlying Bofa basalt outcropping in the eastern side, are gradually lowered down to the west and in the central part of the AVC these units are found at a depth of several hundred meters.

2.2.2 Geology of the study area

The lithologic units that make up the geology of the study area consists of late tertiary silicic volcanic (Nazreth Group) overlain by a unit of fissural flood basalt -Bofa Basalt (Fig. 2.3). The last major event of rift faulting which has occurred in the quaternary age resulted in the formation of so many volcanic complexes called the Wonji Group. The three major volcanic complexes of the Wonji group are the Dino formation, (stratoid silicics of the rift floor), central volcanic complexes, and the fissural basalts of the rift floor. The youngest stratigraphic succession of the study area is the Pleistocene-Holocene age lacustrine sediments, which constitutes most part of the rift floor.

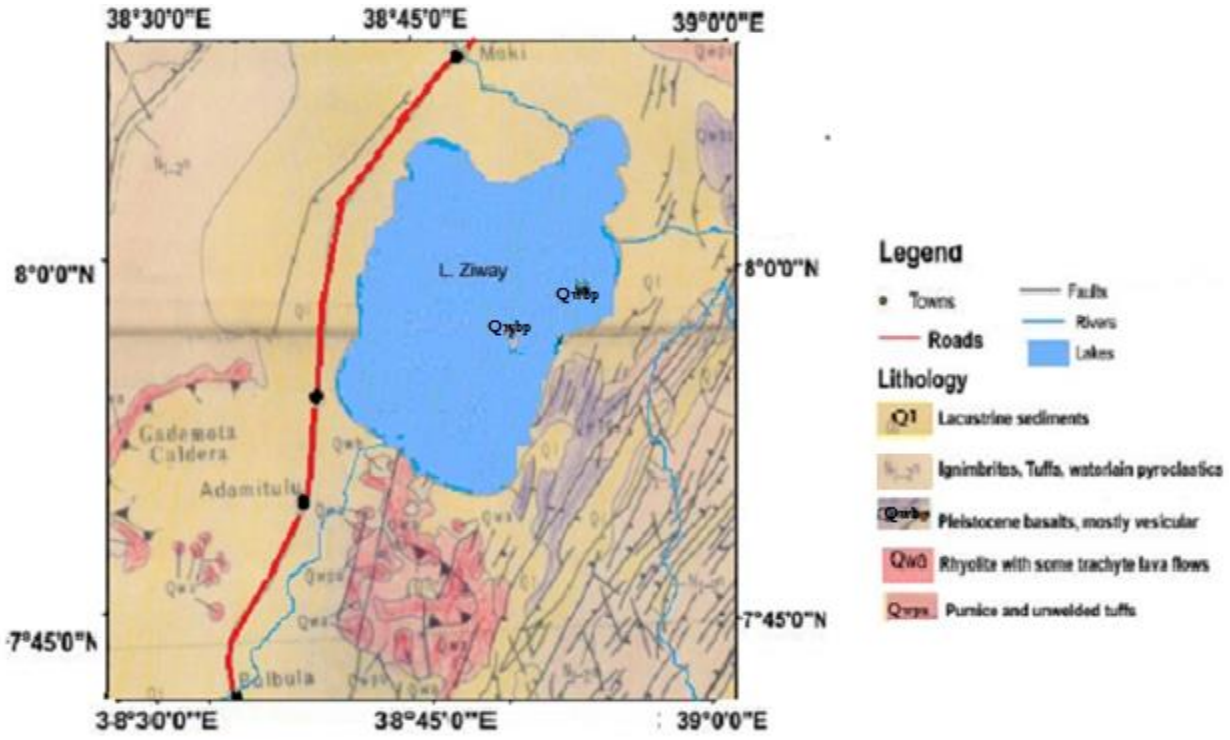

Fig. 2.3 The structural outline and the major lithological units of the study area

(Modified from GSE, 1981)

2.2.2.1 Rhyolite with some trachyte lava flows, pumice and unwelded tuffs (Qwa, Qwpu)

Most of the central volcanoes of the Wonji group are disposed along the axial zone of the rift. They are either huge conical mountains or calderas formed in the place of older volcanoes. The main volcanic centers from north to south within the rift include Aluto. Some occur on the rift floor outside the tensional belts, such as Gademota caldera, or even on the rift shoulders, such as volcanoes and calderas. The main rock types are rhyolitic and trachytic lava flows (Qwa). In some centers alkaline and per-alkaline products are mainly represented by pumice and unwelded tuffs (Qwpu).

2.2.2.2 Pleistocene basalts mostly vesicular (Qwbp)

The bulk of these late basalts are concentrated in the Wonji fault belt, but there are also eruptions in the western marginal part of the rift. The basalts are clearly controlled by extensional fractures and generally display fresh aa surfaces. Chains of scoraceous cones follow the lines of fractures. These basalts are exposed at East of lake Ziway. Recent flows in many cases follow depressions

of relief or flow over fault escarpment. The eruption of basalts usually followed the formation of silicic pantelleritic volcanoes, but some basalt might be contemporaneous with the earliest stages of their development.

2.2.2.3 Ignimbrites, tuffs, under lain pyroclastics, lacustrine beds (N_{1-2}^{n})

The Bofa Basalt and Nazereth Series are in most places overlain by green and gray ignimbrites with well developed fiamme and associated unwelded pyroclastic and underlain pyroclastic with occasional intercalated lacustrine beds and aphyric basalts. The pyroclastics of the Dino Formation may have sources from axial felsic volcanic eruption complexes. The felsic lava of the Dino formation is per alkaline in composition and the ignimbrite members are not confined only to the rift floor but extensively developed on the escarpments.

2.2.2.4 Stratoid silicics: ignimbrites unwelded tuff, ash flows, rhyolites (N1-2n)

In the study area lithologies of stratoidsilicics, ignimbrites, unwelded tuffs, ash flows, rhyolites and trachytes (N1-2n) constitute a considerable portion of the rift escarpments especially in the western part near Munesa town, while in the floor they are unconformably overlapped by younger volcanic of the Dino formation. The time of formation of the Nazareth group is between 9.5 and 3 Ma years (Wolde Gabriel et al., (1990) reported a thickness of more than 600 m for the Pliocene pyroclastic units in the eastern margin of the rift in the Munesa area.

2.2.2.5 Lacustrine Sediments, silts, clays, diatomites (Ql)

In the rift Quaternary sediments and mostly lacustrine origin are intercalated with Pleocene to Pleistocene ignimbrites both in the rift floor and rift shoulders. The older sediments are lacustrine diatomites, tuffaceous clays and silts inter-bedded with basal ignimbrites of the Nazreth Group.

Structures and kinematics of the eastern margin of central Main Ethiopian rift .The lacustrine sediments are intercalated with re deposited volcanic ash and tuffs. The lacustrine sediments are mainly represented by sand and silt. The major components of the sediments are volcanic origin, such as pumice and volcanic ash, obsidian, rhyolite and basaltic rock fragments Bevenuti et al., 2002).

CHAPTER THREE

3 THEORY OF THE GEOPHYSICAL METHODS

3.1 GRAVITY METHOD

3.1.1 General

According to Lillie (1999), Gravity (Derived from Greek word "gravis", which means heavy) is defined as the force of attraction between masses or it is the force of attraction that tends to draw bodies in earth's sphere towards the center of the earth. Gravity survey involves measurements of the gravitational field at a series of different locations over an area of interest. The objective in exploration work is to associate variations with differences in the distribution of densities and hence rock types.

The development of gravity exploration in to its present state has been a result of the contributions of numerous historical accomplishments (Telford et al., 1990). Galileo Galilei's experiment on falling bodies in 1589, formulation of laws of planetary motion by Johann Kepler, discovery of the law of universal gravitation by Sir Isaac Newton , formulation of basic gravitational relationships by Pierre Bouguer, Introduction of compound pendulum by Henry Katar in 1817, extensive gravity surveys using torsion balance in the last of 1920's, development of graphic and grid methods of isolating anomalies in 1940's and calculation of anomalies resulting from simple shapes. Above all, the introduction of digital computers since 1960s has increased geophysicist's capabilities of interpretation of gravity data.

3.1.2 Gravity units

The first measurement of the acceleration due to gravity was made by Galileo in a famous experiment in which he dropped objects from the top of the leaning tower of Pisa (Italy). The c.g.s unit of gravity is called "Gal" which was given in honor of Galileo.

Where: $1Gal = 1cm/s^2 = 0.01m/s^2$

$1mgal = 10^{-3} gal = 10^{-3} cm/s^2 = 10^{-5} m/s2$

Gravity anomalies are very small compared with the mean surface gravity value of 9.81 m/s^2 and are therefore often quoted in a more convenient unit, the milligal, which is equivalent to $10^{-5} m/s^2 (10^{-3}) gal$

3.1.3 Gravity corrections

For most geophysical methods, it is necessary to apply a variety of corrections to the raw data obtained in the field in order to reduce or prepare the data for further enhancement and interpretation (Dentith and Mudge, 2014). In gravity work, more than in any other branch of geophysics, large and in principle calculable effects are produced by sources that are not of direct geological interest (Milsom and Eriksen, 2011).

For example, the value of the observed gravity "gobs "at a given observation point is affected by a number of factors such as the elevation above mean sea level where the point is located, the latitude in which the point is located, the topography of the area in which the measurement is taking place, etc. These effects are removed by reductions that involve the sequential calculation number of recognized quantities. In each case, a positive effect is one that increases the magnitude of the measured field and the sign of the reduction is opposite to that of the effect it is designed to remove (Milsom and Erikson, 2011). This process is known as gravity reduction (Kearey et al., 2002) or reduction to the geoid as the sea level is usually the most common datum level, although the datum plane need not necessarily be the mean sea level (Dobrin, 1988).

Although most corrections are spatial, some are to allow for factors that change the reading when the gravimeter is at the same location (Mussett and Khan, 2000). Drift and Earth Tide correction types are time dependent; whereas the spatial type of corrections are related to variations in distance from the center of the earth. Accordingly, first the time dependent corrections and then the space dependent corrections will be explained next.

3.1.3.1 Instrumental drift correction

The basis for instrumental drift correction arises from the fact that gravimeter reading changes (drifts) with time as a result of elastic creep in the springs, producing an apparent change in gravity at a given station (Reynolds, 1997). Correction for instrumental drift is thus, based on repeated readings at a base station at recorded times throughout the day (Kearey et al., 2002). The base station is commonly revisited at every 1-2 hours (Reynolds, 1997).

The differences between successive measurements at the same station are plotted to produce a drift curve and the observed gravity values from intervening stations can be corrected by subtracting the amount of drift from the observed value (Reynolds, 1997). Drift is assumed to be linear between consecutive base readings (Kearey et al., 2002).

3.1.3.2 Tidal drift correction

Tidal Effect is the variations in gravity observations resulting from the attraction of the moon and sun and the distortion of the earth so produced. Superimposed on instrument drift is another temporally varying component of gravity.

3.1.3.3 Latitude correction

The need for latitude correction arises from two effects (Telford et al., 1990): First, since the earth rotates around its axis and this rotation tends to produce a centrifugal acceleration force, which opposes the effect of the gravitational acceleration. This centrifugal acceleration is maximum at the equator and zero at the poles. Second, due to the imperfect spherical shape of the earth (i.e. flattened at the poles and bulged at the equator), a variation in both equatorial and polar radii arise. This phenomenon gives rise to gravity value variation with distance from the center of the earth.

The latitude correction is thus applied in order to account for these two effects. The average value of gravity for a given latitude (θ) is approximated by the 1967 reference gravity formula, adopted by the International Association of Geodesy (Lillie, 1999).

$$gt = ge(1 + 0.0053\sin^2\theta + 0.0000059\sin^4\theta) \quad (3.6)$$

Where: gt = Theoretical gravity for the latitude of the observation point (mGal); ge = Theoretical gravity at the equator (978031.85 mGal) and θ = Latitude of the Observation Point (Degrees)

3.1.3.4 Free air correction

The need for free air correction (FAC) emanates from the fact that gravity varies inversely with the square of distance from the center of the earth. Hence, it is necessary to correct for changes in elevation between stations to reduce field readings to a datum surface (Telford et al., 1990).

It is the allowance for the reduction of the magnitude of gravity with height from the center of the earth irrespective of the nature of the rock between the observation point and the center of the earth (Reynolds, 1997; Telford et al., 1990).

The change in gravity (Δg) with increasing distance from the center of the earth (ΔR) is given by the first derivative of "g" with respect to "R" (Lillie, 1999):

$$\lim_{\Delta R \to 0} = \frac{\Delta g}{\Delta R} = \frac{dg}{dR} = -2\frac{-2}{R}\frac{GM}{R^2} = \frac{-2}{R}(g)$$

$$\frac{dg}{dR} = \frac{-2g}{R}$$

Assuming average value of g =980.625mGal and R=6.367km=6367.000m

$$\frac{dg}{dR} = \frac{-2g}{R} = -0.308 \text{mGal/m} \qquad (3.7)$$

Where $\frac{dg}{dR}$ = Average value for the change in gravity with increasing elevation

The above equation (3.7) illustrates that for approximately every 3m upward from the surface of the Earth, the acceleration due to gravity decreases by about 1mGal (Lillie,1999).

3.1.3.5 Bouguer correction

Even after elevation correction is made, gravity reading varies from station to station due to differences in mass between the observation point and the sea level datum (Lillie, 1999). The Bouguer correction (BC) is thus, to account for the attraction of material between the station and the datum plane that was ignored in the free air correction (Telford e al., 1990).

Bouguer correction is done by approximating the mass as an infinite slab, with thickness (h) equal to the elevation of the station (Lillie, 1999). The attraction of such slab is:

$$BC = 2\rho rGh \qquad (3.8)$$

Where: BC= Bouguer correction, $\boldsymbol{\rho}$= Density of the Slab, G= Universal gravitational Constant, h = Thickness of the slab. Substituting the values of G and $2\boldsymbol{\rho}$ in equation (3.8) yields:

$$BC = 0.0419\rho h \qquad (3.9)$$

Taking the average crustal density of 2.67 $\frac{\text{g}}{\text{cm}^3}$ and substituting it in the above equation (3.9) yields:

$$BC = 0.112(mGal/m)h \quad (3.10)$$

It can be seen from equation (3.10) that, for every 9 meter of surface elevation, the increased mass below the observation point adds about 1mGal to the observed gravity (Lillie, 1999). The Bouguer correction is subtracted from the observed gravity value if the station is above the datum plane and is added when the station is below the sea level.

3.1.3.6 Terrain correction

The Bouguer correction assumes that the rock occupying the height interval between the datum level and the station is a uniform slab extending to infinity in all directions (Dentith and Mudge, 2014). In other words, the land surface is assumed to be represented by a subdued topography (i.e. the terrain around the observation point is perfectly flat). In reality, there exist "hills" (mountains) rising above the observation point and "valleys" below the observation point.

According to Telford et al., (1990), the terrain correction is thus, to allow for surface irregularities in the vicinity of the observation point. Hills above the elevation of the gravitation station exert an upward pull on the gravimeter, where as valleys (lack of material) below it fail to pull down ward on it. Thus, both types of topographic undulations affect gravity measurements in the same sense as a result of which, the terrain correction is usually added to the observed gravity reading (e.g. Dobrin, 1988; Telford et al., 1990; Reynolds, 1997).

3.1.4 Gravity anomaly

Gravity observations can be used to interpret changes in mass below different regions of the Earth. To see the mass differences, the broad changes in gravity from equator to pole must be subtracted from station observations by predicting the gravity value for a station's latitude (theoretical gravity), then subtracting that value from the actual value at the station (Observed gravity), yielding a gravity anomaly (Lillie, 1999).A discrepancy between the corrected, measured gravity and the theoretical gravity is called a gravity anomaly (Lowrie, 2007). It arises because the density of the Earth's interior is not homogeneous.The most common types of gravity anomalies are the Bouguer anomaly and the free-air anomaly.

3.1.4.1 Free air gravity anomaly

The free air gravity anomaly (ΔgFA) takes in to account the latitudinal change in gravity on theEarth's best fitting ellipsoid represented by the theoretical gravity (gt) and the vertical change ingravity between the reference datum and the observation height assuming that the gravity station is located in free air, hence the name free air anomaly (Hinze et al., 2013).

Lillie (1999) defined free air gravity anomaly as the observed gravity (gobs) corrected for latitude and elevation of the station. The free air anomaly is mathematically calculated as:

$$\Delta gFA = gobs + FAC - gt \quad (3.11)$$

Where: ΔgFA = Free air gravity anomaly; g obs = Observed gravity; FAC = Free air Correction and g t = Theoretical Gravity

From equation (3.11), two things can be understood (Lillie, 1999):

1. Subtracting the theoretical gravity from the observed gravity corrects for the latitude, thusaccounting for the spin and bulge of the earth

2. Adding the "FAC" puts back the gravity lost to elevation, there by correcting the increasedradius "R" from the Earth's center.

3.1.4.2 Bouguer gravity anomaly

The Bouguer gravity anomaly, like the free air gravity anomaly reflects changes in mass distribution below the surface, except the Bouguer anomaly has had an additional correction, removing the effect of mass above sea level datum on land (Lillie, 1999).

The Bouguer gravity anomaly is the most frequently used of the gravity anomalies in surveys ofcontinental and in near shore marine areas (Hinze et al., 2013).

The variation of the Bouguer anomaly should reflect the lateral variation in density such that a high density feature in a lower density medium should give rise to a positive Bouguer anomaly.Conversely, a low density feature in a high density medium should result in a negative Bouguer anomaly (Reynolds, 1997). The simple Bouguer gravity anomaly (ΔgBs) on land is computed from the free air gravity anomaly (Lillie, 1999).

$$\Delta gBs = \Delta gFA - (0.112 mGal/m)h \quad (3.12)$$

Where: h= the elevation in meters.

3.2 Magnetic method

3.2.1 General

Magnetic and gravity methods have much in common, but magnetics is generally more complex and variations in the magnetic field are more erratic and localized (Telford et al., 1990). This is partly due to the difference between the dipolar magnetic field and the monopolar gravity field, partly due to the variable direction of the magnetic field, whereas the gravity field is always in the vertical direction. In addition, magnetic field varies with time whereas gravity field is time invariant (ignoring small tidal variations). Hence, the aim of a magnetic survey is to investigate subsurface geology based on anomalies in the Earth's magnetic field resulting from the magnetic properties of the underlying rocks (Kearey et al., 2002).

Like the gravity method, the magnetic method is a passive geophysical exploration technique in that it is based on mapping the natural or normal magnetic force field of the Earth (Hinze et al., 2013).The aim of a magnetic survey is to investigate subsurface geology on the basis of anomalies in the earth's magnetic field resulting from the magnetic properties of underlying rocks (Kearey et al., 2002).The method has undergone various historical developments. Telford et al., (1990) for example, have compiled the historical perspectives of the method, which is not summarized here. But, above all, the introduction of digital recording and processing of magnetic data and interpretation algorithms have improved the tedious procedures that involve reducing magnetic data in to maps.

Throughout the course of its development, the method has been used for a variety of applicationsranging from Archaeological and Engineering site investigations, to exploration for economicresources and studies of crustal tectonic structures and processes (Hinze et al., 2013).

3.2.2 Nature of Earth's magnetic field

The geomagnetic field at or near the surface of the Earth originates largely from within and around the Earth's core. Magnetic anomalies caused by rocks are localized effects superimposed on the normal magnetic field of the Earth (geomagnetic field) (Kearey et al., 2002). Consequently, knowledge of the behavior of the geomagnetic field is necessary both in the reduction of magnetic data to a suitable datum and in the interpretation of the resulting anomalies. The geomagnetic field

is geometrically more complex than the gravity field of the Earth and exhibits irregular variation in both orientation and magnitude with latitude, longitude and time (e.g., Kearey et al., 2002). Although there are several parts of the geomagnetic field of the earth, the following three are important as far as exploration geophysics is concerned (Telford et al., 1990).

3.2.2.1 The Earth's main field

This field represents the main components of the geomagnetic field and is believed to be originated in the Earth's outer core. This field varies relatively slowly and its magnitude on the earth's surface is given in terms of the geomagnetic field elements (Fig. 3.3).

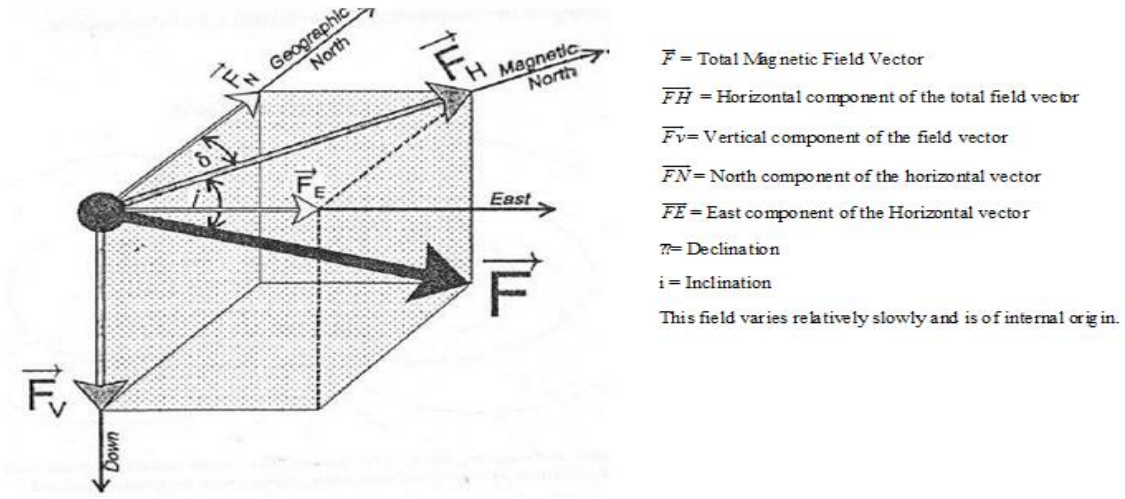

Fig. 3.1 Elements of Earth's magnetic field

(After Tsegay Berhane., 2015)

The total field vector *B* has a vertical component *Z* and a horizontal component *H* in the direction of magnetic north. The dip of *B* is the inclination *I* of the field and the horizontal angle between geographic and magnetic north is the declination *D*. *B* varies in strength from about 25000nT in equatorial regions to about 70000 nT at the poles (e.g., Kearey et al., 2002).

3.2.2.2 The external magnetic field

Most of the remaining small portion of the geomagnetic field appears to be associated with electric currents in the ionized layers of the atmosphere (e.g., Telford et al., 1990). The time variations of this field portion are much more rapid than for the main field and is caused by external activities. Compared to the main field, it varies rapidly and originates outside of the earth.

3.2.2.3 Crustal (anomalous) magnetic field

Local changes in the main field result from variations in the magnetic mineral content of near surface rocks. The sources of local magnetic anomalies cannot be very deep because of the Curie temperature. Thus, local anomalies must be associated with features in the upper crust (e.g., Telford et al., 1990). Generally, the total magnetic field can be expressed by:

$$BT = Bext + B\text{int} = Bext + BD + Brm \quad (3.13)$$

Where BT is the total magnetic field, Bext is external magnetic field, BD is dipole field, which is mainly generated by the fluid outer core and Brm is the field of rock magnetism.

3.2.3 Temporal variations of earth's magnetic field

3.2.3.1 Secular variations

These are longer period variations of the Earth's magnetic field of usually greater than a year (Mudge and Dentith, 2014). Although their mechanism is not understood well, several theories indicate that they are due to changes in electric currents producing the internal field (e.g. Dobrin and Savit, 1988; Mudge and Dentith, 2014).

There are also variations in the inclination and declinations of the field; in which the geomagnetic field of the earth has reversed its polarity a number of times in the geologic time as revealed from a number of paleomagnetic studies, with the most recent one occurred about 700000 years ago (Mudge and Dentith, 2014).

3.2.3.2 Diurnal variations

These are smaller but more rapid oscillations in the earth's field with a period ranging about a day and amplitude averaging 25 Gamma (Dobrin and Savit, 1988).

They are due to changes in the external field related to sources external to the earth. These are chiefly due to electric currents flowing in the ionosphere, the ionized layer of the upper atmosphere, and are associated with radiation from the Sun (Dentith and Mudges, 2014). They are of direct significance to magnetic prospecting.

3.2.3.3 Magnetic Storms

These are rapid variations of the field with periods of milliseconds to minutes appearing as irregular bursts lasting from hours to several days (Dentith and Mudges, 2014). Magnetic surveying must stop in such events, as they occur so rapid and in unpredictable way that correcting their effects is not feasible (Dobrin and Savit, 1988).

They correlate with sun spot activity and cause a wide range of amplitude changes, up to 1000nT at most latitudes and even greater at the poles (Dobrin and Savit, 1988).

Magnetic storms make magnetic surveying impractical because the target anomalies related to the crustal rocks are often smaller in amplitude than these erratic variations (Dentith and Mudges,2014)

3.2.4 Magnetization and magnetic susceptibility of materials

3.2.4.1 Magnetization

If a body is placed in an external magnetic field (also called inducing field), it acquires although usually small, a magnetization which is proportional to the inducing field (Milsom, 2003). The relationship is given as:

M$\boldsymbol{\alpha}$H

(The magnetization acquired is directly proportional to the induced field)

$$M = \alpha H$$

Where M =Magnetization acquired by the material; $\boldsymbol{\alpha}$=Magnetic susceptibility of the material;

H =Inducing field

3.2.5 Measuring magnetic field strength and measuring Instruments

According to Dentith and Mudge (2014), magnetic objects alter the strength and direction of the Earth's magnetic field. Changes in the field's direction due to most geological features are very small and offer very little resolution in detecting variations in the magnetic properties of the subsurface. However, the effect on field strength is significant and is by far the most sensitive element to changes in the magnetic properties of crustal rocks.

It is the strength of the magnetic field that is measured and mapped in magnetic surveying.

Although a number of devices have been developed and used since the first century AD, magnetometers used specifically in exploration geophysics can be classified in to three categories (Reynolds, 1997). These are: the torsion (and balance); Fluxgate and Resonance types, of which the first has been superseded by the latter two.

The resonance type magnetometers are also classified in to the proton Precession magnetometer and Alkali- vapor magnetometer, both of which monitor the precession of atomic particles in anambient magnetic field to provide an absolute measure of the total magnetic field (Reynolds, 1997).

The proton precession magnetometer (usually abbreviated as proton magnetometer) measures the total strength of the magnetic field, but not its direction and so shows a total field anomaly, also called a total intensity anomaly (Mussette and Khan, 2000).

The fluxgate magnetometer on the other hand, measures the strength of magnetic field in a particular direction. As a result of which, the fluxgate magnetometer is in essence a vector magnetometer and finds applications where the direction to a magnetic source is required, such as down hole magnetometer and down hole electromagnetic (Dentith and Mudge, 2014).

3.2.6 Magnetic data reduction

The reduction of magnetic survey data is principally aimed at removing the effects of temporal variations in the Earth's magnetic field that occur during the course of the survey. Like gravity reduction, planetary-scale spatial variations in the field are compensated for, but in contrast, elevation-related variations in the magnetic field are minor.

As the Earth's magnetic field varies from nearly 25,000nT at the magnetic equator to 69000nT at the poles, the increase with magnitude needs to be taken in to account (Reynolds, 1997). Survey data at any given location can be corrected by subtracting the theoretical field value (Fth), obtained from the International Geomagnetic Reference Field (IGRF) from the measured observed value (Fobs)

To remove all causes of magnetic variation from the observations other than those arising from subsurface geology it is necessary to make a correction to the magnetic raw data.

3.2.7 Magnetic data Correction

3.2.7.1 Diurnal variation correction

The effects of diurnal variation may be removed in several ways. On land, the magnetometer is read at a fixed base station periodically throughout the day. The differences observed in base readings are then distributed among the readings at stations occupied during the day according to the time of observation. Magnetometers do not drift and base readings are taken solely to correct for temporal variation in the measured field (Kearey et al., 2002).

3.2.7.2 Geomagnetic correction

In order to produce a magnetic anomaly map of a region, the data have to be corrected to take in to account the effect of latitude and to a lesser extent longitude (Reynolds, 1997). Survey data at any given location can be corrected by subtracting the theoretical field value Bth, obtained from the International Geomagnetic Reference Field (IGRF) from the measured value, Bob. Therefore, the magnetic anomaly (ΔB), obtained by subtracting the diurnal correction (σD) and geomagnetic correction (Bth) is given by:

$$\Delta B = BT - \delta BD - Bth \quad (3.1)$$

CHAPTER FOUR

4 DATA ACQUISITION, REDUCTION AND PROCESSING

4.1 General

The present thesis work has utilized gravity and magnetic methods. The data for gravity method is secondary in that it was obtained from previously collected sources (sections 4.2.1). On the other hand, the magnetic data are partly primary which were collected by the researcher and his advisor during the field season (February 2018) and partly secondary which were collected by different individual researchers.

All the gravity and magnetic data utilized in this work were collected in a random distribution fashion. The selection of the survey patterns in effect has taken the accessibility of study area, scale of the study, time and financial constraints and others in to account.

In both of the above methods, the field measurements have been recorded using a field recording format in at least three attributes (geographic coordinates in terms of Easting and Northing, Elevation or height above sea level) and the anomaly reading associated with each geophysical method employed. Accounts of the data acquisition and consequent reduction processes associated with each geophysical method are summarized below.

4.2 The Gravity Data

4.2.1 Gravity data acquisition

As mentioned in section (4.1), all the gravity data used in the present work amounting to 862 in number as depicted in the gravity data location plot map (Fig. 4.1); were obtained from secondary sources, namely; the work of Abera Alemu (1992) and Geological Survey of Ethiopia (GSE).

The secondary data obtained from both sources as cited in their reports were collected using the Lacoste and Romberg gravimeter within the limits of accuracies suggested for geological studies which range from 1 - 0.01 mGal (Hinze et al., 2013).

The location in terms of Easting, Northing, and height above mean sea level of the respective observation points for all the secondary gravity data were determined using classical surveying techniques and a handheld Global Positioning System (GPS).

As far as the survey design is concerned, all the gravity data obtained from both sources were collected in a random type of survey pattern, with station spacing varying from 2 to 5 kms on average and the gravity data distribution is shown in Figure 4.1.

4.2.2 Gravity data reduction

Gravity observations include the combined effects of instrumental, surface, terrain and planetary sources in addition to the subsurface lateral mass variations that are the objective of an exploration gravity survey (Hinze et al., 2013). The gravity data reduction processes in the present work thus, were aimed at transforming the raw data sequentially into a data table of final complete Bouguer anomaly values by correcting the variations in the earth's gravitational field, which do not result from the differences of density in the underlying rocks.

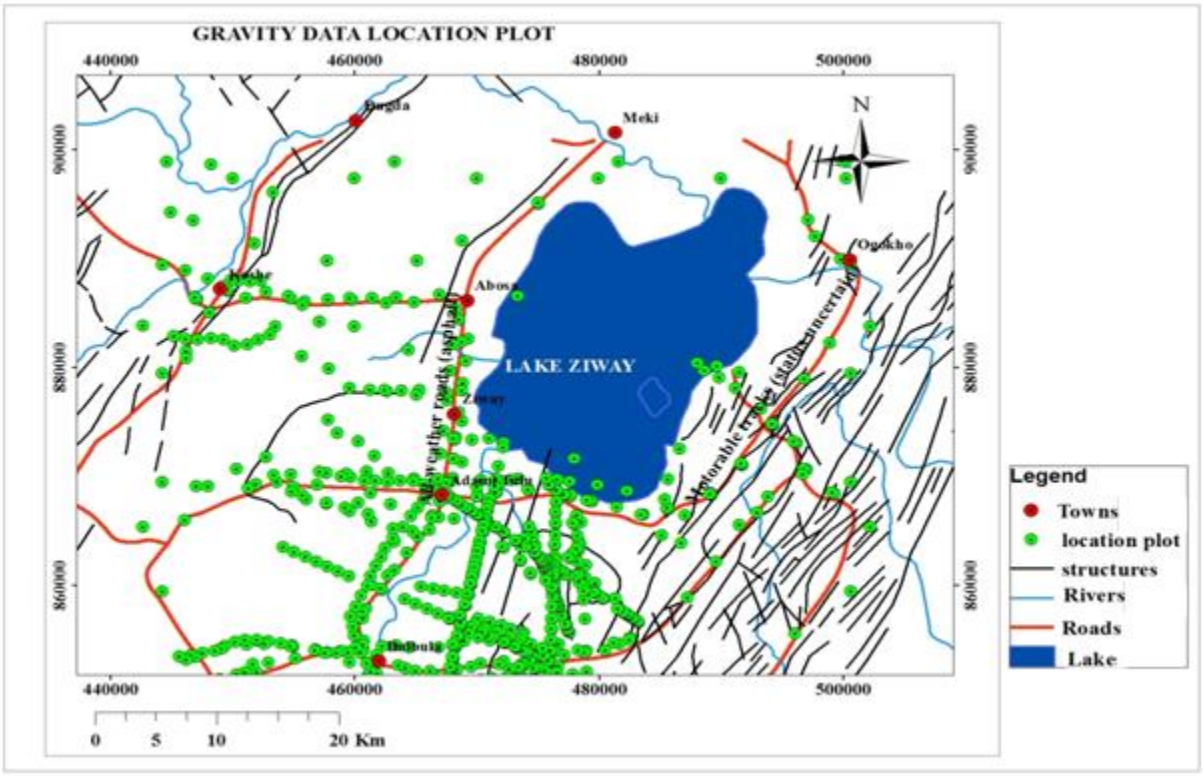

Fig. 4.1 Gravity data distribution map of the study area

4.3 The magnetic data

4.3.1 Magnetic data acquisition

The magnetic data points utilized in the present thesis work amounts to a total of 304 as shown in the magnetic data location plot map (Fig. 4.2). The data consists of primary data collected by the

researcher and secondary data obtained from previous surveys. Both the primary and secondary data are measured by using proton precision magnetometers. This type of magnetometers measure the total intensity of earth's magnetic field at a given observation point, with an accuracy of one Gamma claimed by the manufacturers.

The surveys were conducted randomly with the geographic coordinates and elevation of each observation point determined using a hand held GPS apparatus (Garmin 12).

Before any measurement was made, a base station for all the measurement stations occupied was established for correcting the diurnal effect. Accordingly, both the primary and secondary magnetic data were made available for further reduction and processing steps.

The data density distribution (Fig. 4.2), over the study area is variable, with very low data density around Lake Ziway and relatively denser data points over the Aluto volcanic center.

4.3.2 Magnetic data reduction

Reduction of magnetic survey data principally aims at removing the effects of temporal variations in the earth's magnetic field that occur during the course of the survey, usually the diurnal and secular effects (Tsegay Berhane, 2015).

Accordingly, both the primary and secondary magnetic data were corrected for diurnal and secular effects following two main reduction phases: Diurnal corrections to the observed total magnetic field intensity at all the observation stations was computed using an empirical diurnal correction formula, which is not discussed here. IGRF corrections calculated using the Geosoft oasis montaj software (V.7.0.1) for the year 2005 was subtracted from the diurnally corrected values to get the total magnetic field anomaly values of all the stations occupied.

The computed total magnetic field anomaly values were then used to compile the total magnetic field anomaly map (Fig.5.6), and its derivative maps, which include the regional magnetic anomaly map (Fig.4.4), and the residual magnetic anomaly map (Fig.4.5).

Consequent processing and enhancements were based largely on the residual magnetic field anomaly map generated using the continuation filtering techniques applied in Oasis Montaj

(v.7.0.1).

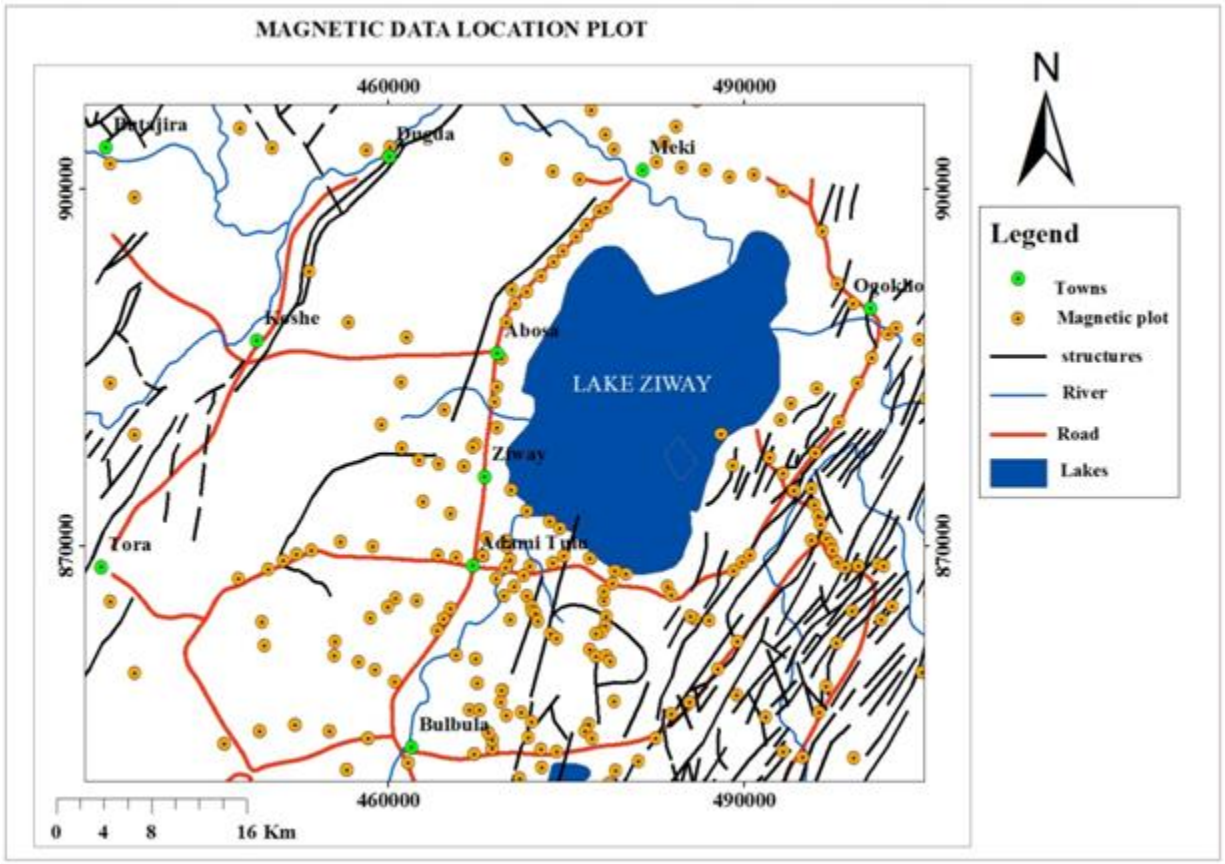

Fig. 4.2 Magnetic data distribution map of the study area

4.4 Data processing and presentations

4.4.1 Gravity data processing and presentations

In the present thesis work, after the necessary reductions and allowances for the effects like latitude, elevation, slab and terrain have been made to the raw gravity data (Section 3.1.). The complete Bouguer anomaly and its derivative anomalies have been computed using the Geosoft gravity and magnetic data processing and mapping software Oasis Montaj V 7.0.1

In this thesis work, the computed point gravity anomaly values were gridded using the minimum curvature gridding method in order to interpolate the field data in to a regular, square grid using an average grid cell size of 10000 m. A complete Bouguer anomaly map (Fig. 5.1) was finally generated by using the complete Bouguer anomaly value column as gridding column, which was used then as the final gravity anomaly map base for further enhancements (filtering) and

interpretations. The complete Bouguer anomaly map (Fig. 5.1) generated represents the sum of the regional (deep seated) and local (residual) anomalies which arise from responses of the large, deep seated and local, shallow depth geologic materials and structures, respectively. Hence, there is a need to separate the responses of both regional and local features from the complete Bouguer anomaly data for effective and better interpretations of the intended research objectives.

Accordingly, following the gridding and complete Bouguer anomaly map generation step, the residual and regional anomaly separation process of the gravity data was accomplished using the low and high pass filtering methods using Geosoft Oasis Montaj Software (V 7.0.1). Accordingly, the regional gravity anomaly map (Fig 5.2) was generated using the Geosoft OasisMontaj Software by subtracting the residual gravity anomaly data from the complete Bouguer anomaly data.

After the separation of the residual and regional anomalies, different data enhancements and filtering techniques have been applied including respective maps such as Horizontal gradient map (Fig. 5.4) and Euler depth solutions for SI= 0.5 (Fig. 5.5) are generated, discussed and interpreted.

4.4.2 Magnetic data processing and presentations

The magnetic data utilized in the present work have undergone through series of data reduction steps before they were subjected to the data processing and presentations phases.

Hence, corrections on the daily variations (Diurnal correction) and the effect of the core field (IGRF) removal from the measured (Observed) total magnetic intensity anomaly values have resulted in total magnetic anomaly values. It was the IGRF corrected anomaly values taken as a final and base anomaly values for generating the IGRF corrected anomaly map using the Geosoft Oasis Montaj Software (V 7.0.1) in which, further enhancements, filtering operations and interpretations have been based.

The total magnetic anomaly map (Fig. 5.7), like the complete Bouguer anomaly map (Fig 5.1) in the gravity survey, represents the sum of the effects of the shallow depth, short wave length and deep seated, long wavelength source effects. Hence, effective interpretations of the magnetic data necessitate the separation of the regional and residual responses from the IGRF corrected total magnetic intensity anomaly values.

Following the separation of the regional and residual magnetic anomalies using the same procedures as applied in the gravity data, further filtering techniques and enhancements were performed as per the procedures of the magnetic data processing steps.

The end result of the gravity survey (complete Bouguer anomaly values) computed at all the stations considered in the study area are plotted at their specific locations to the complete Bouguer anomaly map (Fig. 5.1) of the study area using the Geosoft OasisMontaj software.

CHAPTER FIVE

5 Results and Interpretation

5.1 Complete Bouguer anomaly map

The compiled complete Bouguer anomaly map (Fig. 5.1) indicates that the gravity responses reflect the heterogeneity in the subsurface density distribution beneath the survey area.

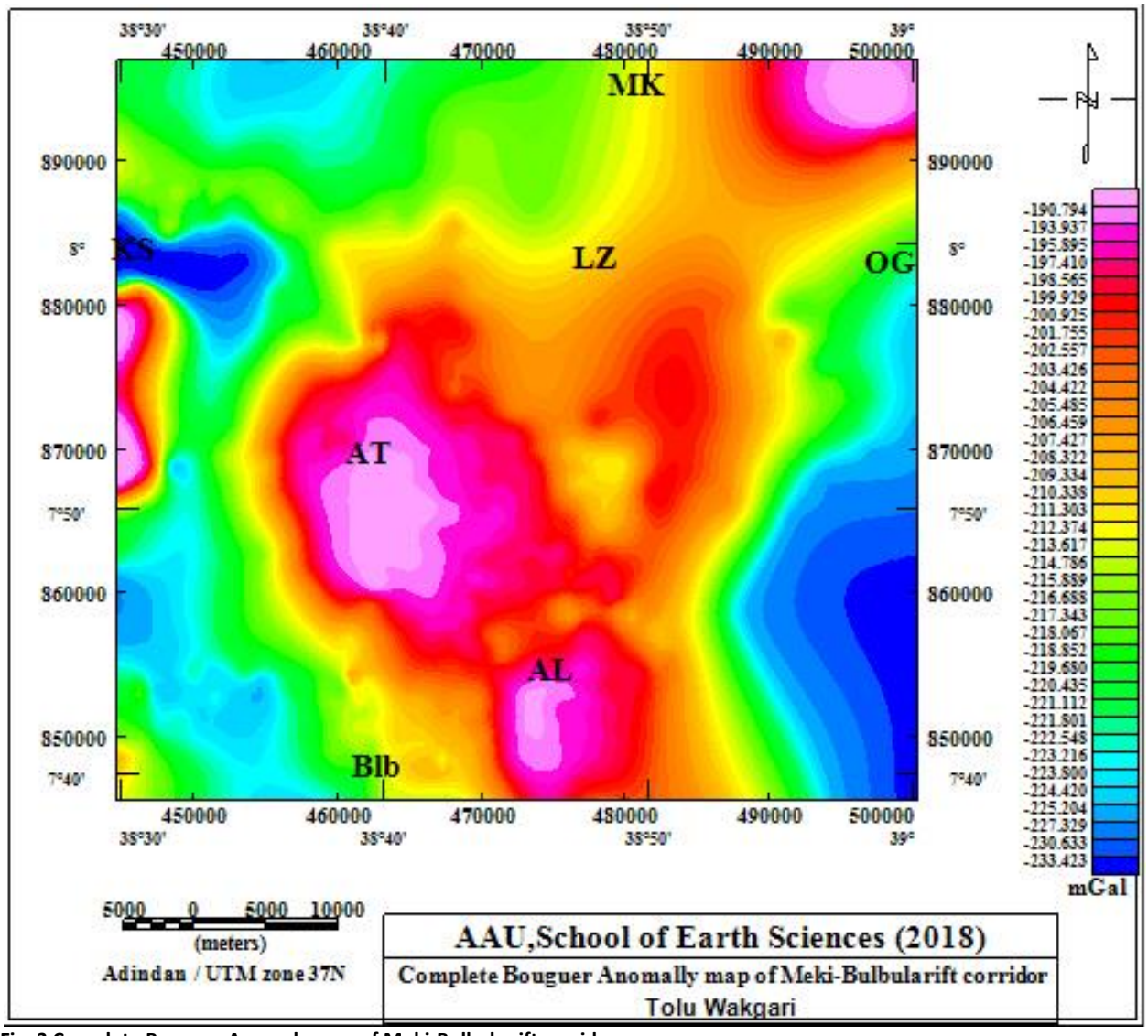

Fig. 3 Complete Bouguer Anomaly map of Meki-Bulbula rift corridor

(Where: AL: Aluto volcanics, AT: Adami Tulu, Blb: Bulbula, KS: Koshe, LZ: Lake Ziway, MK: Meki, OG: Ogolcho)

The values of the observed gravity anomaly in the study area range from a minimum of -233.4 mgal to a maximum of -190.8 mgal. The anomaly map further reveals two distinct anomaly zones, which include the medium to very high central positive anomaly zone which is oriented in a NNW - SSE direction and a medium to very low negative anomaly zones located in the North western, eastern, south western and south eastern part of the study area.

The positive peak (-190.8 mgal) which corresponds to the location of the Aluto volcanic centre is thought to be caused by high-density volcanic products (rhyolite, trachyte, etc.) observed on the geologic map (Fig.2.3) of the study area. The positive peak (-190.8 mgal) which corresponds to the location of the Adami Tulu locality is thought to be caused by high-density rhyolite intrusions observed on the geologic map (Fig.2.3) of the study area and also noted during field observations.

5.1.1 Regional gravity anomaly map

The complete Bouguer anomaly map consists the sum of the effects of features of long wave length, deep seated (regional anomaly) and the near surface, short wave length (residual anomaly) components. Separation of these components is important to determine the effects of the deep-seated and the shallow depth sources contributing for the complete Bouguer anomaly.

Despite the availability of various methods of anomaly separation, a low pass filtering with a cutoff wavelength 15 km was applied to the complete Bouguer anomaly for generating the regional Bouguer gravity anomaly using Geosoft Oasis Montaj (V 7.0.1) based on the following series of steps.

During filtering, increasing the separation between the source and detector causes a decrease in amplitude and increase in wave length of the response, where the rate of attenuation of amplitude is wave-length dependent (i.e. Shorter wavelengths, high frequencies associated with near-surface sources attenuate more rapidly with height than the longer wavelengths and lower frequency sources. Hence, shorter wavelength, shallow- sourced responses plus any short wave length noises are suppressed and longer wavelength responses dominate the filtered data (Dentith and Mudges, 2014)

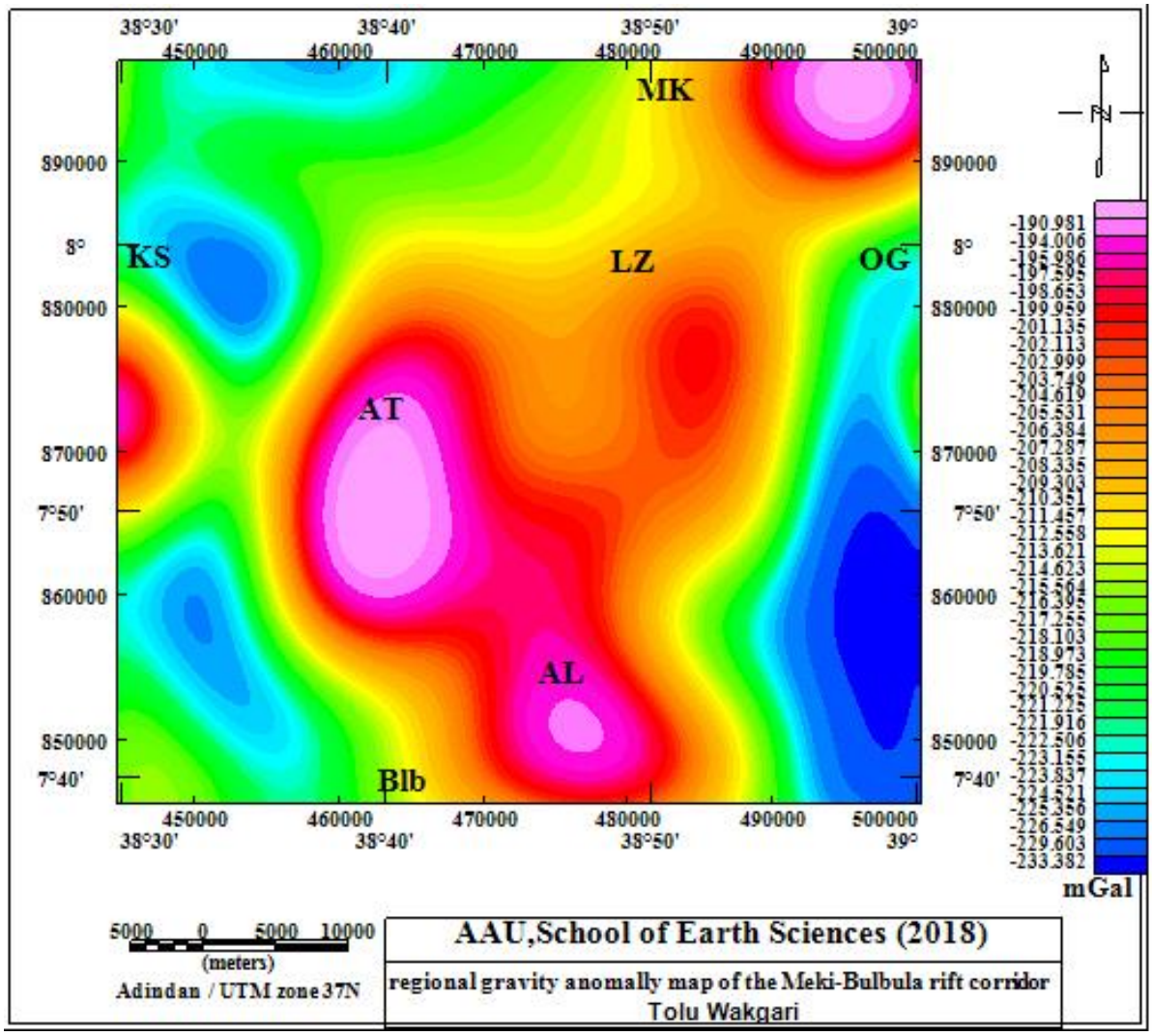

Fig. 5.4 Regional gravity anomaly map of Meki-Bulbula rift corridor

(where: AL: Aluto volcanics, AT: Adami Tulu, Blb: Bulbula, KS: Koshe, LZ: Lake Ziway, MK: Meki, OG: Ogolcho)

The Regional anomaly map (Fig. 5.2) reveals three prominent anomaly zones, which are similar to those of the complete Bouguer anomaly map (Fig. 5.1). The anomaly map further reveals two distinct anomaly zones, which include the medium to very high central anomaly zone which is oriented in a NNW to SSE direction and a medium to very low negative anomaly zones located in the North western, eastern ,south western and south eastern part of the study area. The only difference between them is that the anomaly features observed in regional anomaly map are smooth and elongated indicating that they are the effects of deep seated anomalous geologic structures. As this MSc thesis work is concerned with investigating shallow subsurface structures, a detailed interpretation of the regional gravity anomaly map is not considered here.

5.1.2 Residual gravity anomaly map

The residual gravity anomaly map (Fig. 5.3) was generated after the separation of the regional Bouguer gravity anomaly value from the complete Bouguer anomaly value using the high pass filtering methods with a cutoff wavelength 15 Km using Geosoft Oasis montaj software (V 7.0.1).

The residual gravity anomaly map (Fig. 5.3) reveals the gravity anomalies resulting from shallow depth anomalous geologic structures in the subsurface.

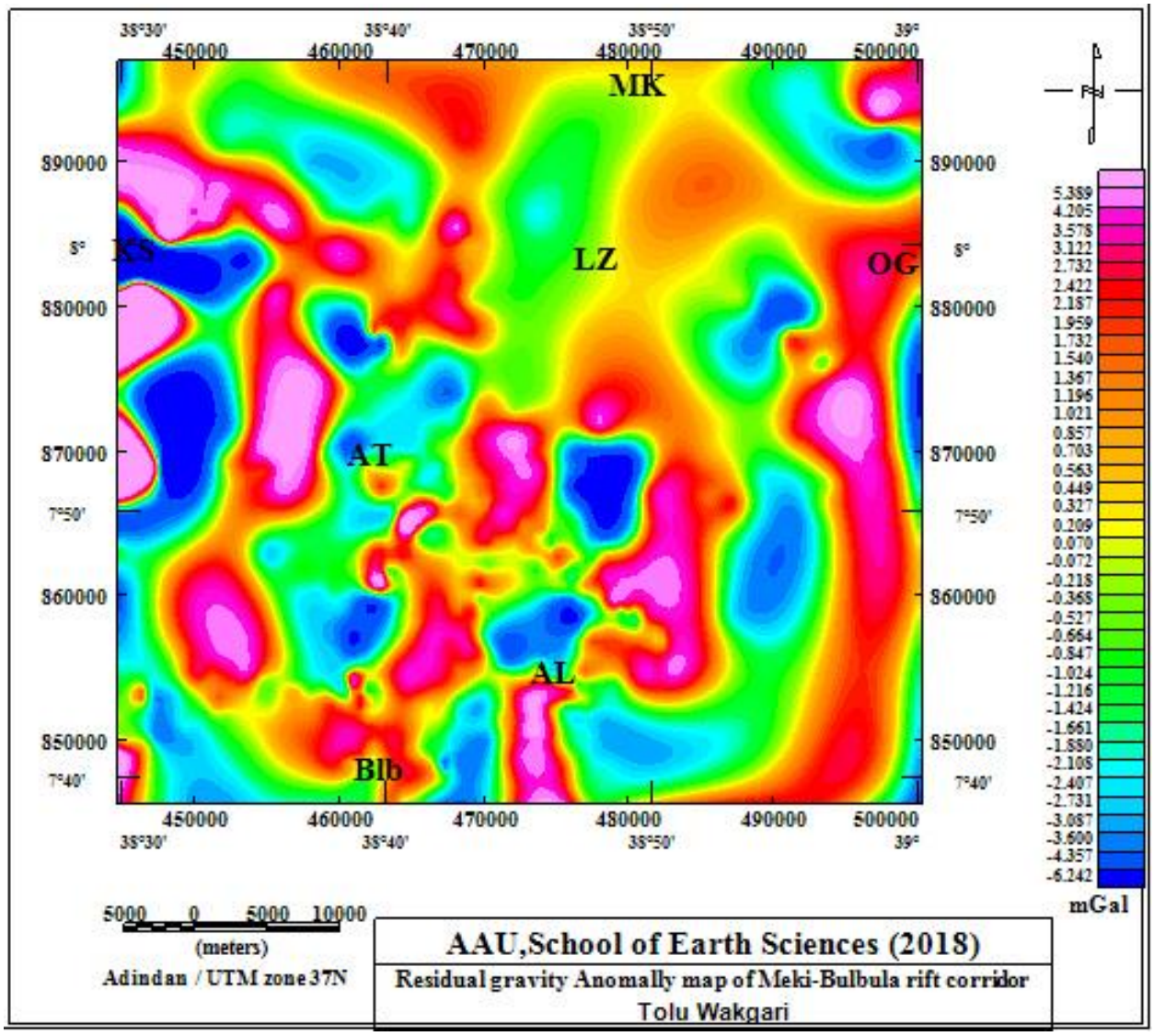

Fig. 5.5 Residual gravity anomaly map of Meki-Bulbula rift corridor

(Where: AL: Aluto volcanics, AT: Adami Tulu, Blb: Bulbula, KS: Koshe, LZ: Lake Ziway, MK: Meki, OG:Ogolcho)

The residual gravity anomaly map is dominated by a number of positive and negative short wave length anomalous features aligned almost in N-S and NW-SE directions. The maximum anomaly peaks in the study area coincide with the locations of high-density volcanic products of the Aluto volcanic center, Gademota caldera and Ogolcho locality. The high anomaly zone which runs in a N-S direction in the central and eastern parts of the study area are thought to be caused by high density volcanic materials occurring along the Wonji Fault Belt (WFB).

The circular to elliptical local lows, which appear to be surrounded by the highs ovaer the central part of the study area could be the expression of thick accumulation of the rift floor sediments and water bodies filling Lake Ziway.

The low anomaly which is surrounded by the highs of the Aluto high density volcanic products is interpreted as the effect of low density sediments deposited over the Aluto caldera and the associated volcanic ash and the pyroclastic materials composing the Aluto volcano (Fig.2.2).

5.1.3 Horizontal gradient gravity map

The horizontal gradient is a mathematical anomaly enhancement method that can be computed by:

$$HG = HG(x, y) = \sqrt{(\frac{\partial \Delta g}{\partial x})^2 + (\frac{\partial \Delta g}{\partial y})^2}$$

Where Δg is the residual anomaly,

The horizontal gradient (HG) method is used to locate the boundaries of regions of contrasting density. The method is based on the premise that the maximum horizontal gradient of the observed gravity anomaly, which is caused by a planar anomalous body, tends to overlie the edges of the body. Note also that the edges mark locations of the contacts indicating that the HG method is designed to inspect fault and contact features.

The horizontal gradient gravity map (Fig. 5.4) is produced from the residual gravity anomaly grid using the Geosoft Oasis Montaj software (V7.0.1). The map reveals horizontal gradients maxima that are anticipated to indicate locations and where linear structures (faults, fractures) are dominantly occurring in the study area. The orientations of the horizontal gradients are thought to indicate directions of weak zones that favor the flow direction of groundwater at shallow depths. The map reveals lineated maximum horizontal gradient anomalies, which are oriented in the SW-

NE direction in the northwestern part of the study area. The central part of the study area is dominated by oriented horizontal gradients with different orientation directions.

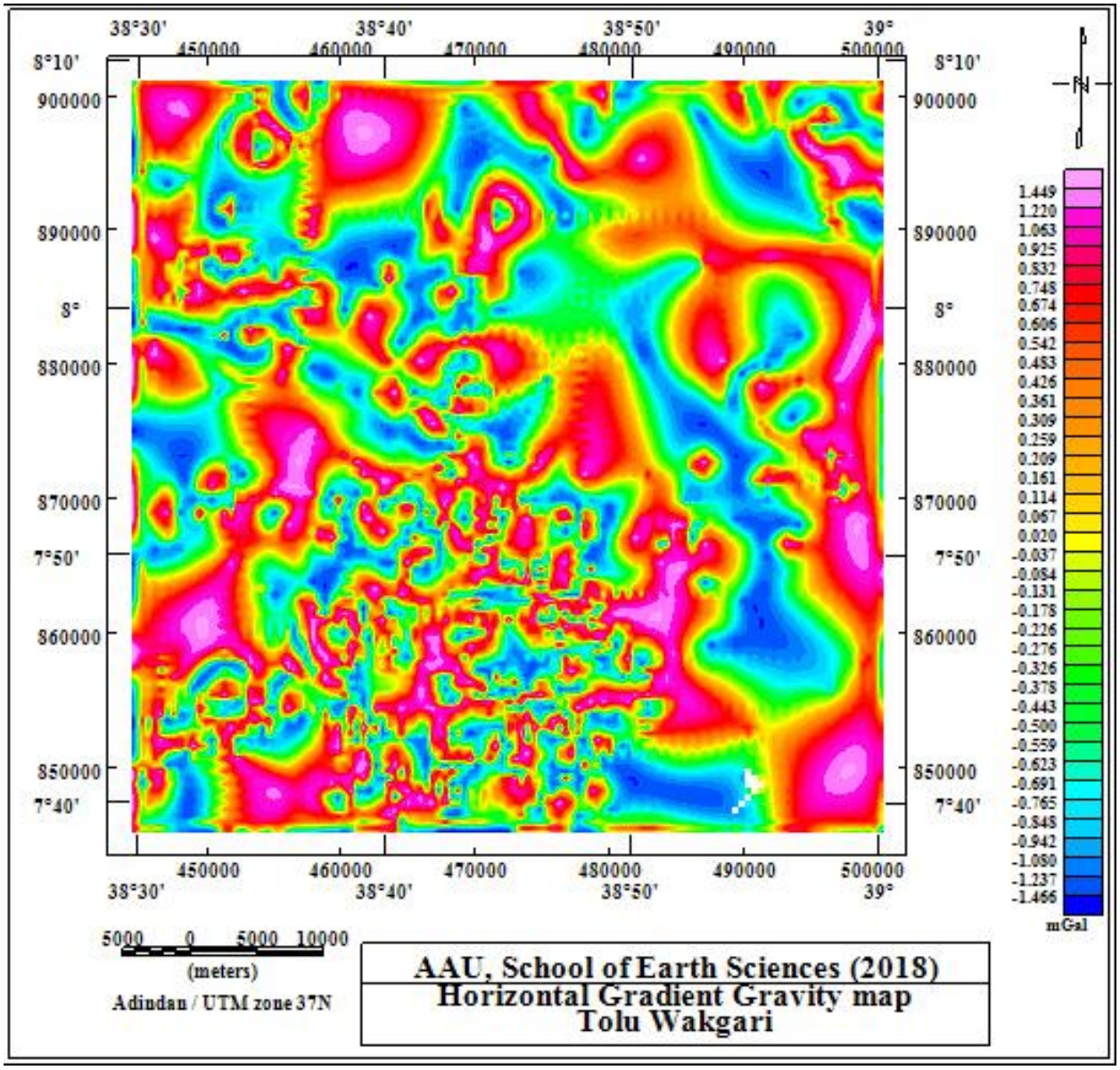

Fig. 5.6 Horizontal Gradient gravity map of the study area

Locations of the maximum horizontal gradient magnitude are shown with black lines superposed along their orientation (Fig. 5.5). The high horizontal magnitude plots outline lateral mass heterogeneities which are thought to be the expressions of lithological and structural boundaries. The high gradient magnitude plots trace linear features trending N-S, the linear features are attributed to faults and fractures, and their continuities are observed in the study area. Moreover the N-S trending linear features (faults and fractures) revealed by the horizontal gradient map can

be considered to be the major geologic structures that favor the flow of ground water from lake Ziwayto Lake Langano(Fig. 5.5).

5.1.4 Euler deconvolution gravity map

The Euler deconvolution gravity data enhancement method is used to estimate location, depth and nature of geologic sources generating the anomalies. The Euler deconvolution equation, which is thought to operate for gravity data in 3D, was developed by Reid *et al* (1990) given by:

$$(x-xo)\frac{\partial \Delta g}{\partial x}+(y-yo)\frac{\partial \Delta g}{\partial y}+(z-zo)\frac{\partial \Delta g}{\partial z}=n(\beta-g)$$

Where (x_0, y_0, z_0) is the position of a source (source location) whose gravity anomaly of preference is computed at (x, y, z), β is the regional gravity anomaly value, and n is the structural index (SI), which can be defined as the rate of attenuation of the anomaly with distance. The SI must be chosen using prior knowledge of the source geometry. For example, SI = 2 for a sphere, SI = 1 for a horizontal cylinder, SI = 0 for a fault, and SI = –1 for a contact.

The Euler deconvolution method is applied to the residual gravity data in order to estimate the depth and location of the shallower (subsurface) anomalous sources. Accordingly, the Euler deconvolution gravity map (Fig. 5.6) of the study area is produced for a structural Index (SI= 0.5). The structural index (SI= 0.5) is chosen based on the objective of the survey, which is mapping the areal distribution and depth wise variation of linear structures (faults and fractures) found in the study area.

Euler solutions obtained from the residual gravity data show well clustering over the area of Meki-Bulbula rift corridor. This clustering confirms the minor faults as shown in the geologic map of the study area and infers new faults in different directions at different depths. Combining these results in one tectonic map could give a clear image of the subsurface structure of the area of Meki-Bulbula rift corridor.

The Euler deconvolution gravity map (Figure 5.6) shows that high clustering of the depth solutions for SI=0.5 are values associated with linear structures at depth levels ranging from 1.6 to 2.1 km whose locations are plotted on the map with an inverted triangle shaded with dark blue, light blue, green, yellow and red colors. The map shows linear structures:

- at depths less than 1.6 km by the dark blue inverted triangles. The location of these linear structures is dominantly concentrated at the southern central part of the study area at about the southern and southwestern parts of the Aluto volcanic complex.

- at depths between 1.6 to 1.8 km by the light blue inverted triangles with

- at depths between 1.8 to 2 km by the green inverted triangles

- at depths between 2 and 2.1 km by the yellow inverted triangles

- at depths greater than2.1 km by the red inverted triangles

- Inverted triangles with light blue colors indicate linear structures with depths from 1.6 to 1.8 km regions of intense faulting, fracturing and extensional activities.

The map reveals locations of sources at different depths marked by colored symbols.

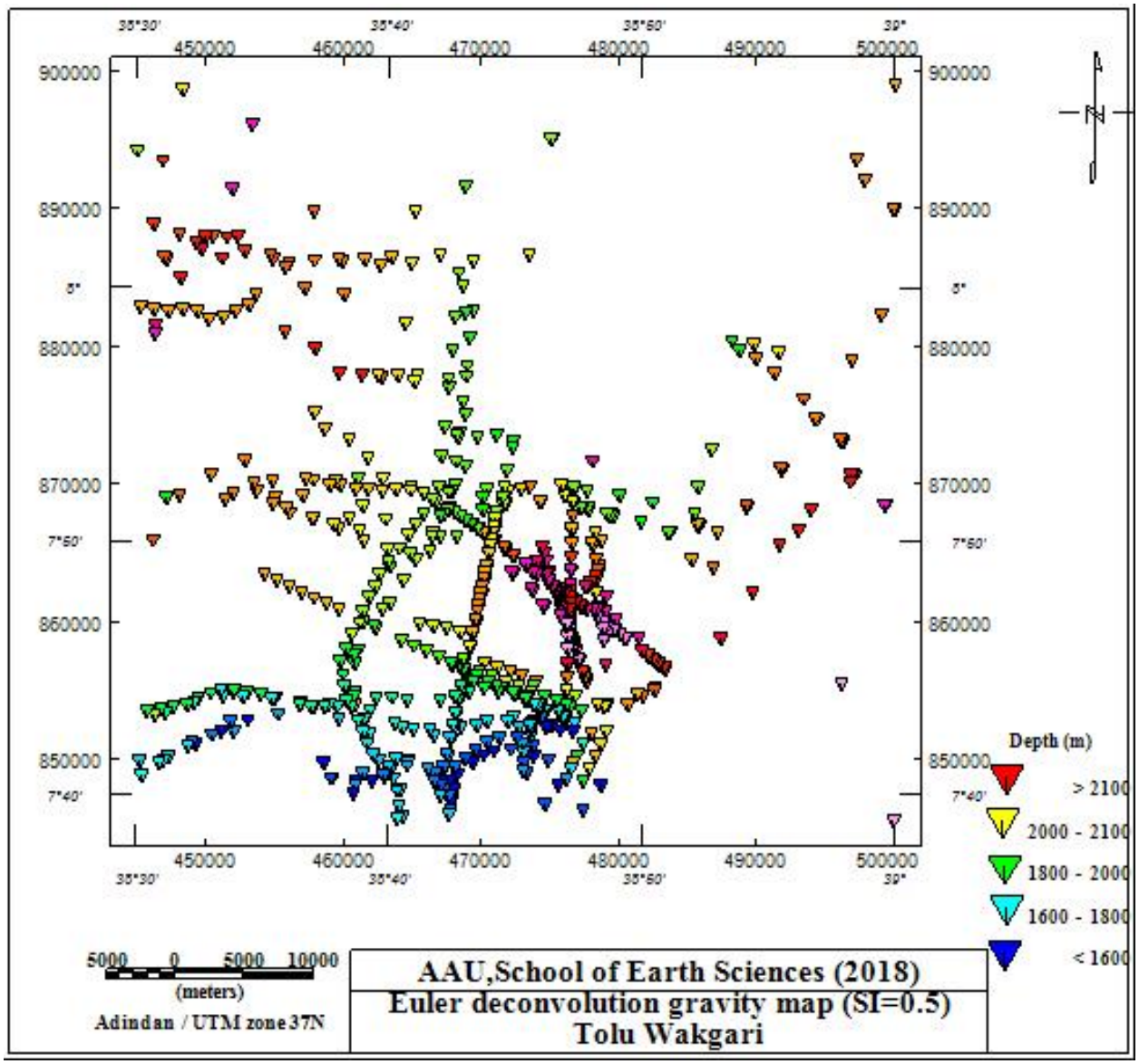

Fig. 5.7 Euler deconvolution gravity map of the study area

5.2 Magnetic Data Results and Interpretation

5.2.1 Total magnetic field anomaly map

The total magnetic anomaly map (Fig.5.7) compiled for the study area shows anomaly values ranging from -391.5 to 294.6 nT. The eastern, central, south eastern, western and north western parts of the study area are characterized by high magnetic anomaly values ranging from 50-294.6 nT.

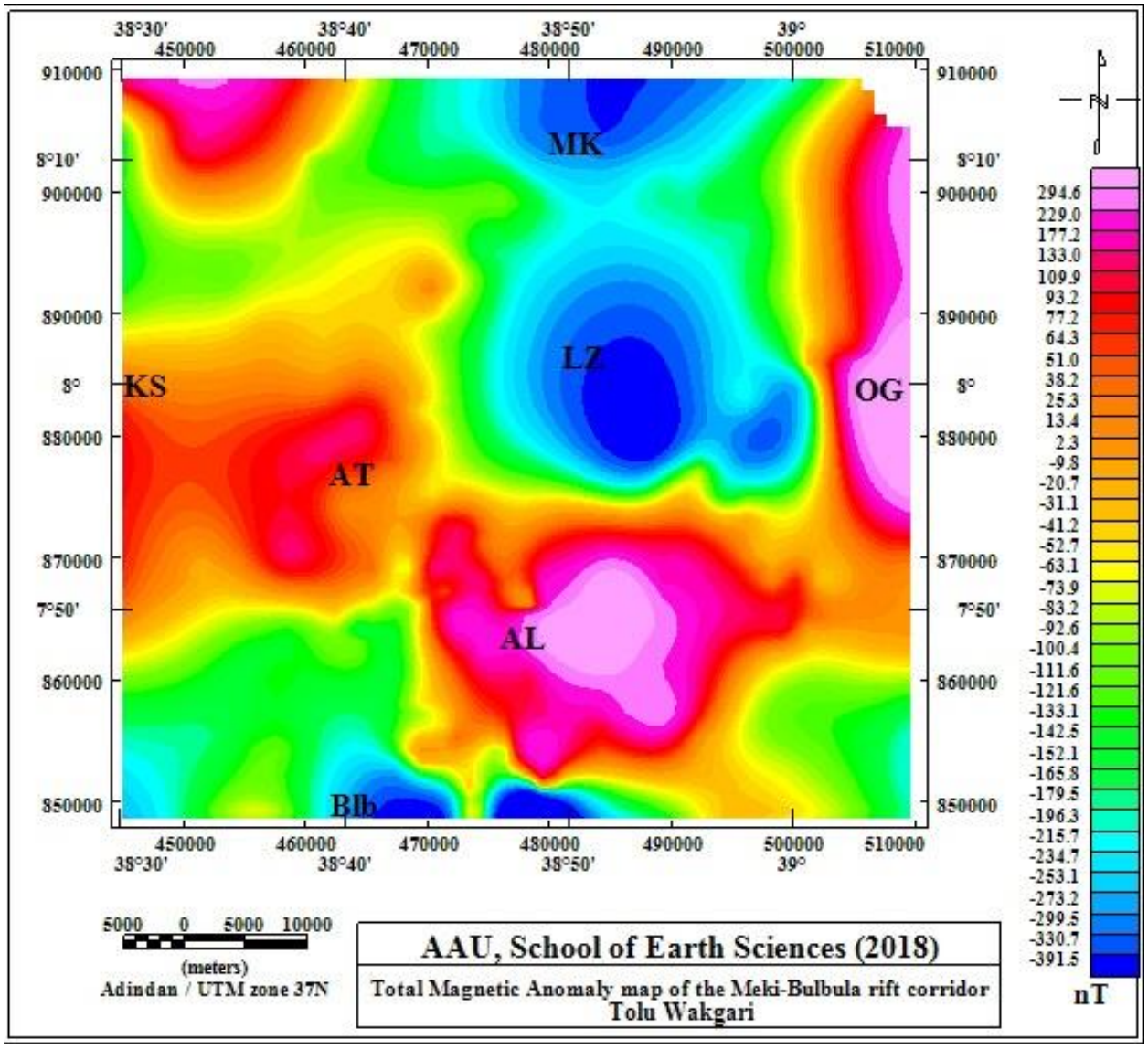

Fig. 5.8 Total magnetic field anomaly map

(Where: AL: Aluto volcanics, AT: Adami Tulu, Blb: Bulbula, KS: Koshe, Mk: Meki, OG: Ogolcho)

The high magnetic anomaly (295nT) observed over the central part of the map labelled, coincide with the locations of the Aluto volcanic center. The high magnetic anomalies recorded which are observed in the North and NW part of the study area indicate the existence of pyroclastic materials in the area and the effect of nearby linear features like faults and fractures of the surrounding area. Eastern and SE parts of the area are associated with a series of faults and pyroclastic materials and Aluto volcanic center, respectively. The largest part of the mapped area is characterized by medium to very low total field magnetic anomaly values. These include medium and low anomaly areas

close to the volcanic centers of the region as located on the slopes of the volcanic centers in the Aluto volcanic centers and sediments of the rift floor, respectively.

Very low total magnetic anomaly values characterize the Northeastern, most part of the Central, and southern part of the study area. These areas are relatively low lands in the study area, most of which are filled with lacustrine sediments bearing low susceptibility values and are largely covered by the lake of the area, mainly Lake Ziway.

5.2.2 Regional magnetic field anomaly map

The regional magnetic anomaly map of the study area was generated after low pass filtering technique with a cutoff wavelength 20 km has been applied to the Total Magnetic Field Anomaly using the Geosoft Oasis MontajSoft ware (V.7.0.1).

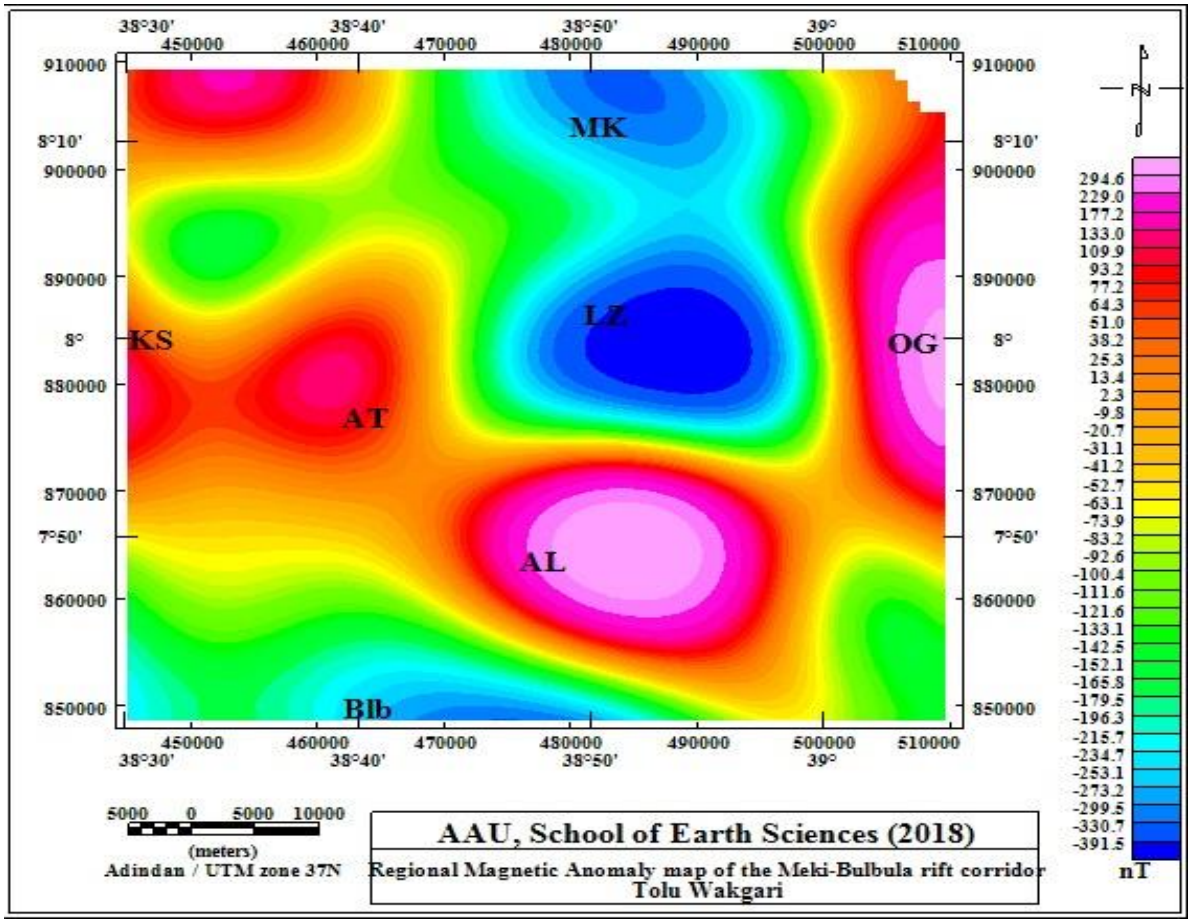

Fig. 5.9 Regional magnetic anomaly map of the Meki-Bulbula corridor

(Where: Al: Aluto volcanics, AT: Adami Tulu, Blb: Bulbula, Ks: Koshe, Mk: Meki, Og: Ogolcho)

A general steady increase in magnetic anomalies southwards from the South/SW part of the study area, with the Eastern, central SE, Western and North Western part characterized by high to very high anomalies are observed in the study area. The magnetic susceptibility of geologic materials may explain the observed regional increase in the magnetic anomaly, high magnetic anomaly readings being interpreted as the responses of low magnetically susceptible earth materials, as observed with the silicic volcanic centers of Aluto in the study area.

5.2.3 Residual magnetic field anomaly map

The residual magnetic anomaly map (5.9) was generated after the separation of the regional anomaly from the total magnetic Field data. The map depicts subsurface features in detailed manner better than those revealed by the observed total magnetic field anomaly map. High to very high residual anomalies characterize to the Eastern, Southern and some of the Northern parts of the study area. The very high residual anomalies observed in the area are in the form of mostly patches and elongated features.

As described on the map, the central, southwestern and some of the northern part of the study area are mostly characterized by low to very low magnetic anomaly values. These regions are largely occupied by the Lake Ziway and the surroundings, which is filled with Quaternary sediments in most of the central parts.

It is determined that there is an inverse relationship between magnetic susceptibility behavior of geologic materials and their magnetic anomaly responses in equatorial areas. As the present study area is located very close to the magnetic equator, the high magnetic anomaly observed over the volcanic complexes are associated with the low susceptibility volcanic materials that resulted from the high heat flow associated with the volcanoes. (In other words, the observed high magnetic anomalies over the volcanic complexes are due to low susceptibility materials that are magnetized by the earth's equator magnetic field).Areas covered by basaltic rocks are associated with positive magnetic anomalies as observed at Eastern of Lake Ziway which may result from high remanent magnetization.

Conversely, the observed negative anomalies could be thought to result from the relatively high susceptibility sedimentary rocks (not affected by high heat flow) derived from the neighboring volcanic complexes

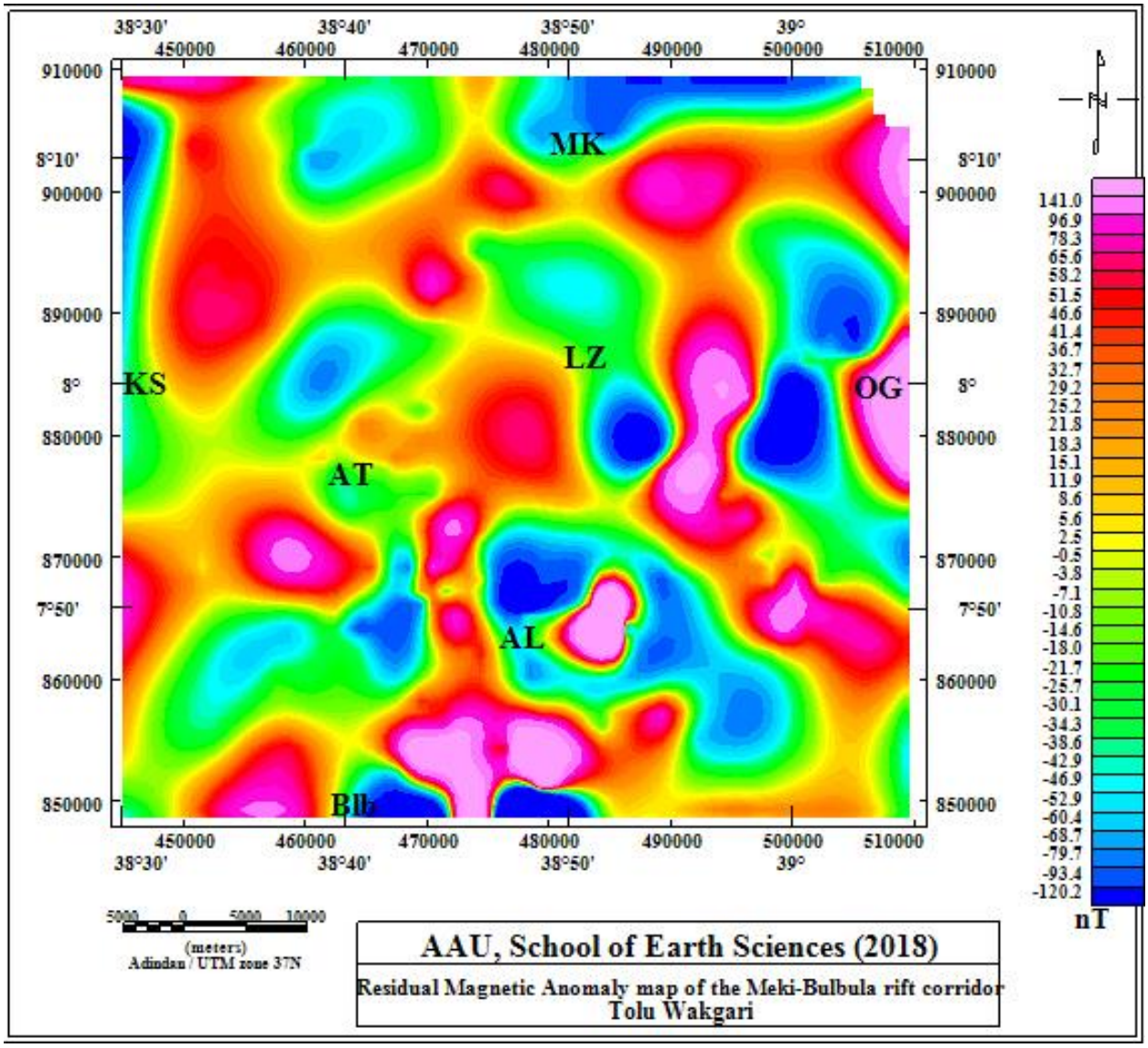

Fig. 5.10 Residual Magnetic Anomaly map of Meki-Bulbula rift corridor

(Where: AL: Aluto volcanics, AT: Adami Tulu, Blb: Bulbula, KS: Koshe, LZ: Lake Ziway, MK: Meki, OG: Ogolcho)

5.2.4 Analytical signal (total gradient)

The Analytical signal of a potential field, such as magnetic field, is generated by combining the 3-directional gradients of the potential field at location (X,Y) in use and is given by the following formula (Dentith and Mudges, 2014).

$$AS(x,y) = \sqrt{(\frac{\partial \Delta B}{\partial x})^2 + (\frac{\partial \Delta B}{\partial y})^2 + (\frac{\partial \Delta B}{\partial y})}$$

Where, ΔB is the residual magnetic anomaly field

The Analytical signal has the form of the ridge located above the vertical contact and is slightly displaced when the contact is dipping with the crest of the ridge delineates the edge of the top surface.The width of a maximum or ridge is an indicator of depth of the contact, as long as the signal arising from a single contact can be resolved (GETECH Group Plc., 2007)**.** The analytic signal maxima occur directly over the edges of source bodies. The analytic signal is peaked over the location of the top of the contact.

The analytical signal map of the study area is generated after performing analytical enhancement filtering on the residual magnetic anomaly map already produced. As can be seen from the map (Fig.5.9), forms of ridges, with magnetic anomaly peaks are observed on the NE, SW and central part of the mapped area. These observations seem to coincide with the magnetic anomaly highs identified in the residual magnetic anomaly map. These zones are also coincident with the zones where magmatic intrusions are associated with.

Hence, there are two evident structural contacts identified (indicated by the thick white broken lines, Fig. 5.9), with a general trend of NW- SE and NE –SW, with the majority of these structural contacts aligned in a NW – SE trend.

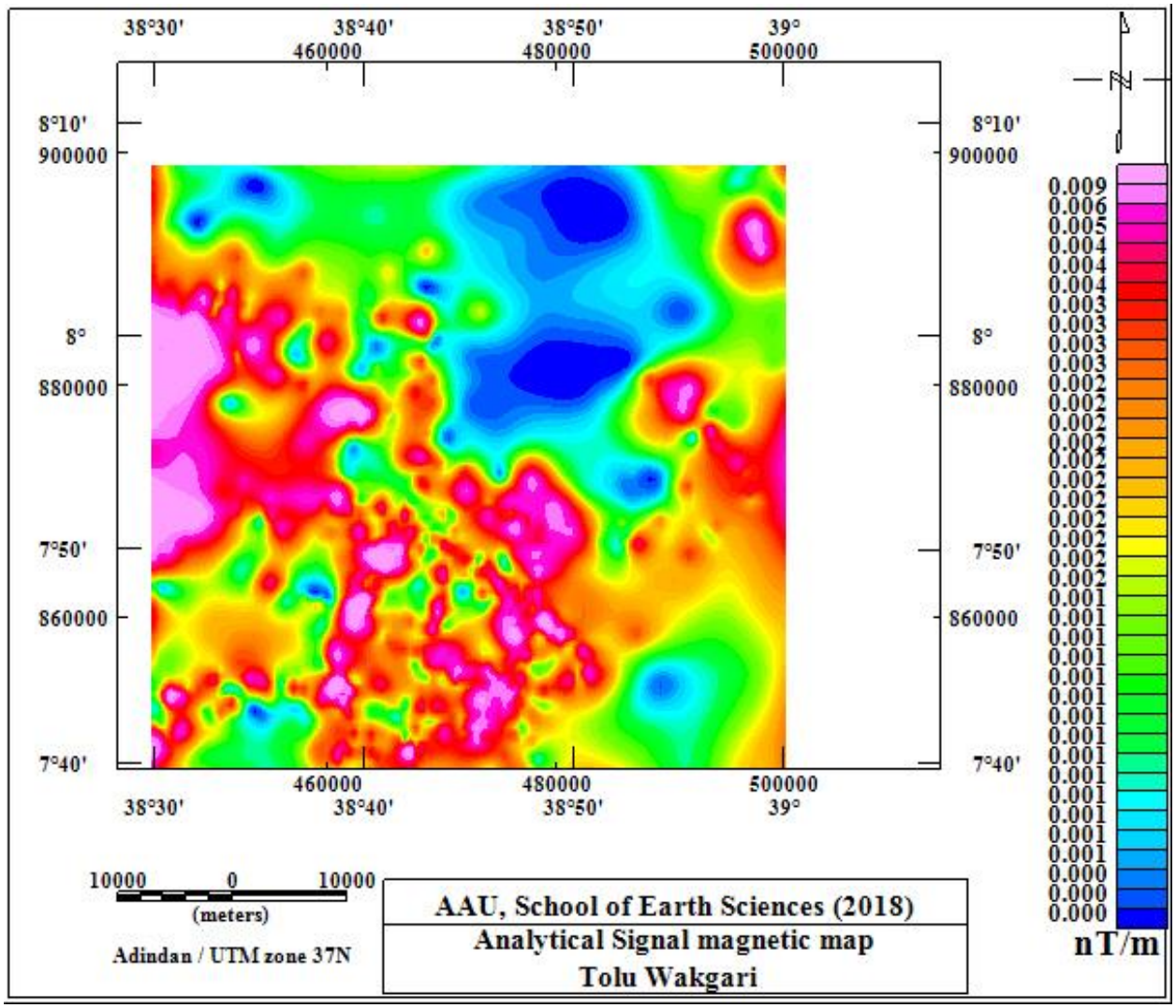

Fig. 5.11 Analytical Signal magnetic map

(Where: Al=Aluto volcanics, AT=Adami Tulu, Blb=Bulbula, Ks=Koshe, Mk=Meki, Og= Ogolcho)

5.2.5 Tilt derivative magnetic map

The Tilt Derivative maps are used to locate the edges/boundaries of geologic structures prevailing in a given study area. In the present work, the Tilt

Derivative map generated as depicted in (Fig. 5.10), shows a more refined and detailed structural contacts/ boundaries (as delimited by the black broken lines, Fig. 5.10), than was observed in the residual magnetic anomaly map and its counter analytical signal map. According to the rules of interpretations of Tilt Derivative Maps, zero contour values marked by yellow line on the map correspond to the contact or boundaries of geologic structures. As can be seen from the Tilt

Derivative Map generated in the present work, the study area is characterized by numerous structures delineated by contact/boundaries. The result is in good agreement with the geologically studied surface results that the study area has been subjected to extensive faulting and fracturing activities over the course of its geological history.

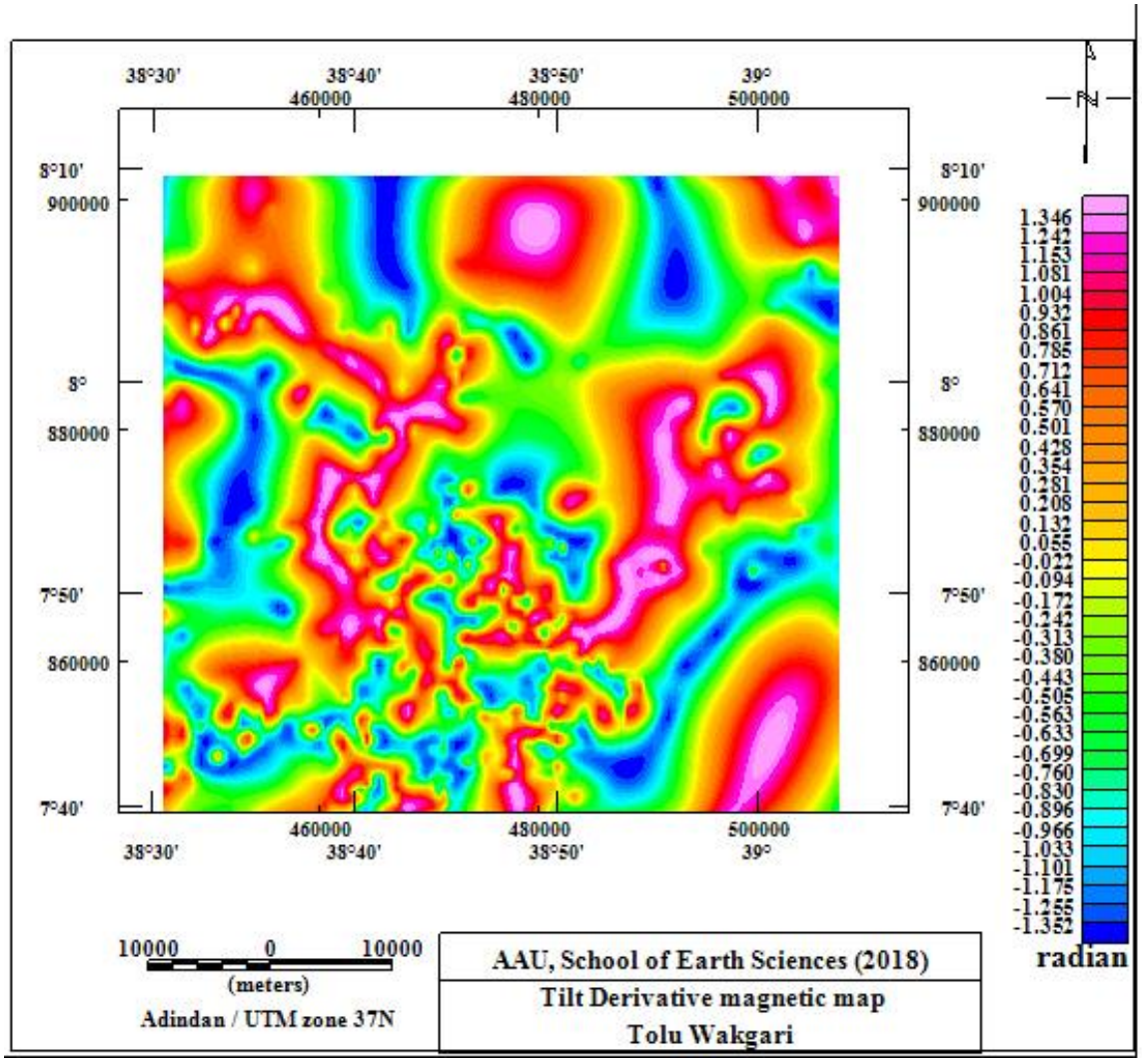

Fig. 5.12 Tilt Derivative magnetic map of Meki-Bulbula rift

5.2.6 Euler deconvolution magnetic maps

The magnetic Euler depth maps like that of their gravity counter parts show that the prevailing geological features are located close to the surface with a depth range of less than ten kilometers. The clustering of the depth solutions again show similar trend of locations as in the gravity Euler depth maps (Fig. 5.12). The Euler deconvolution method is applied to the residual magnetic data

in order to estimate the depth and location of the shallower (subsurface) anomalous sources. Accordingly, the Euler deconvolution magnetic map (Fig. 5.12) of the study area is produced for a structural Index (SI= 1). The structural index (SI= 1) is chosen based on the objective of the survey, which is mapping the areal distribution and depth wise variation of linear structures (faults and fractures) found in the study area.

Euler solutions obtained from the residual magnetic data show well clustering over the area of Meki-Bulbula rift corridor. This clustering confirms the minor faults as shown in the geologic map of the study area and infers new faults in different directions at different depths. Combining these results in one tectonic map could give a clear image of the subsurface structure of the area of Meki-Bulbula rift corridor.

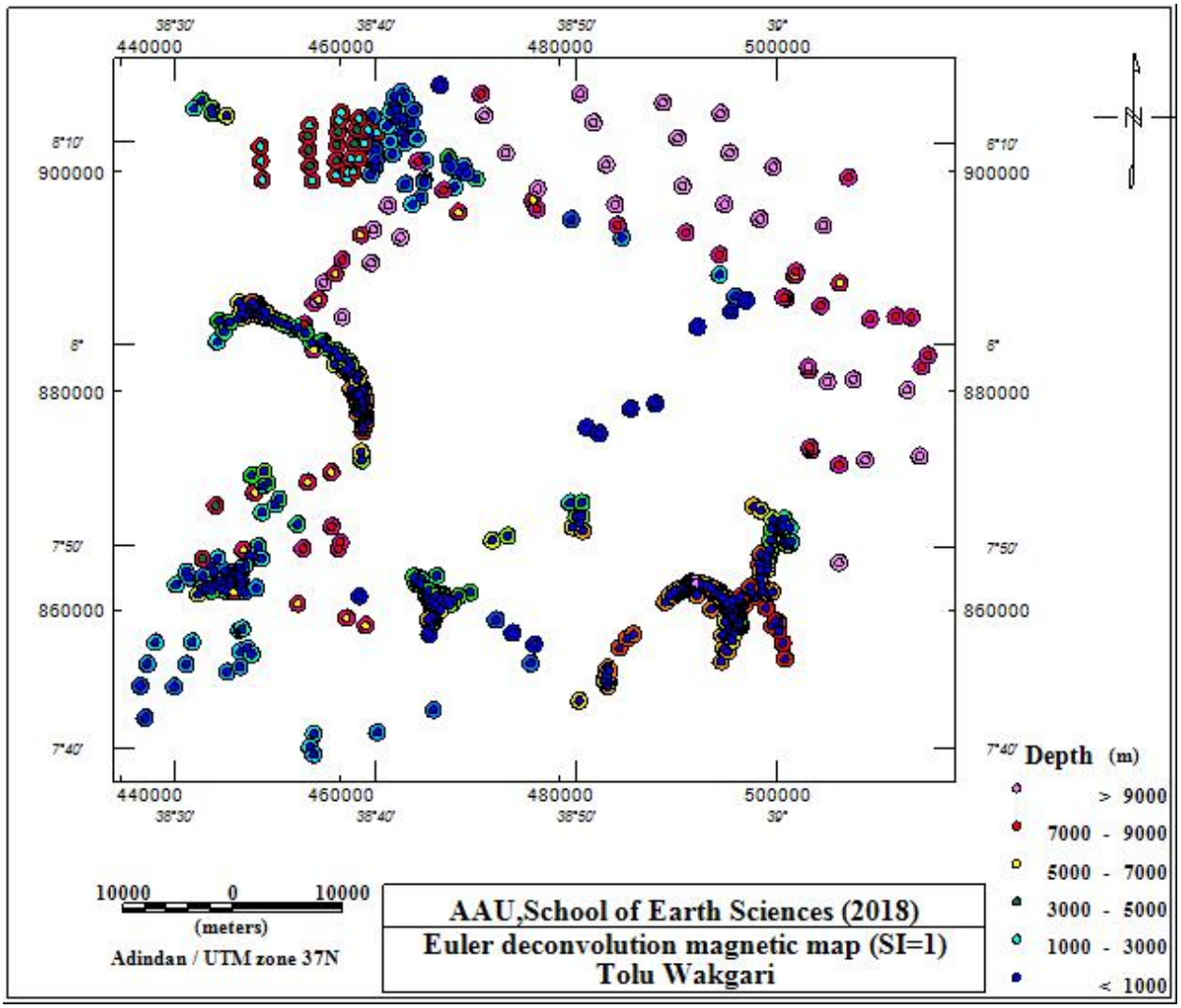

Fig. 5.13 Euler deconvolution magnetic map of the study area

The Euler deconvolution magnetic map (Fig. 5.11) shows that high clustering of the depth solutions for SI=0 are values associated with linear structures at depth levels ranging from 1 to 9 km whose locations are plotted on the map with circles shaded with dark blue, light blue, green, yellow , red and pink colors. The map shows linear structures:

- at depths less than 1km by the dark blue circles. The location of these linear structures is dominantly concentrated at the SW, central, northern and NW parts of the study area at the southern and southwestern parts of the Aluto volcanic complex.

- at depths less than 1 km by the dark blue circles

- at depths between 1to 3 km by the light blue circles

- at depths between 3 to 5 km by the green circles

- at depths between 5 and 7 km by the yellow circles

- at depths between 7 and 9 km by the red circles

- at depths greater than 9 km by the pinkish circles

- Circles with light blue colors indicate linear structures with depths from 1 to 3 km regions of intense faulting, fracturing and extensional activities.

The map reveals locations of sources at different depths marked by colored symbols.

5.3 Combined qualitative interpretation of the gravity and magnetic survey results

In the study area, most of the high anomaly responses from the geophysical methods utilized in the present work show a close correlation in delineating the subsurface geologic structural features beneath localized zones. The observed comparatively positive anomalies largely occur at the locations of the volcanic complexes. In contrast, the observed relatively negative geophysical

anomaly responses appear to be associated with the areas that lie adjacent or away from the volcanic complexes, particularly close to the shores of Lake Ziway and Lake Langano.

In qualitative terms, the gravity highs (refer to the different gravity anomaly maps under section 5.1) and the magnetic highs (refer to the different magnetic anomaly maps under section, 5.2)

considered in the study area are associated with the zones that are characterized by the volcanic centers.

The gravity highs and magnetic highs are exclusively linked with the volcanic centers of Aluto in the North/NE in the Central sections of the study area.

Interpretations of the geophysical responses vary from one method to another, as far as resource exploration, particularly subsurface structure is considered, the geophysical survey tools seeks to delineate the gravity and magnetic methods are used to delineate the subsurface structures which favor for the formation of ground water.

The gravity and magnetic highs in almost all of the maps generated (depicted under sections 5.1 and5.2), are associated with the Aluto volcanic complex in the study area.

All the geophysical investigation results leads to the conclusion that the shallow depth subsurface structures identified beneath the study area control the ground water flow from Lake Meki to Bulbula.

5.4 2D Gravity modeling

To give a tentative quantitative interpretation regarding the subsurface lithological units of the study area a 2D gravity modeling was constructed along profile P1and profile P2 (Fig 5.13) in the study area.

The gravity models are prepared from the residual Gravity anomaly map (Fig. 5.4) using the Geosoft Oasis Montaj GM-SYS 2Dmodeling software.

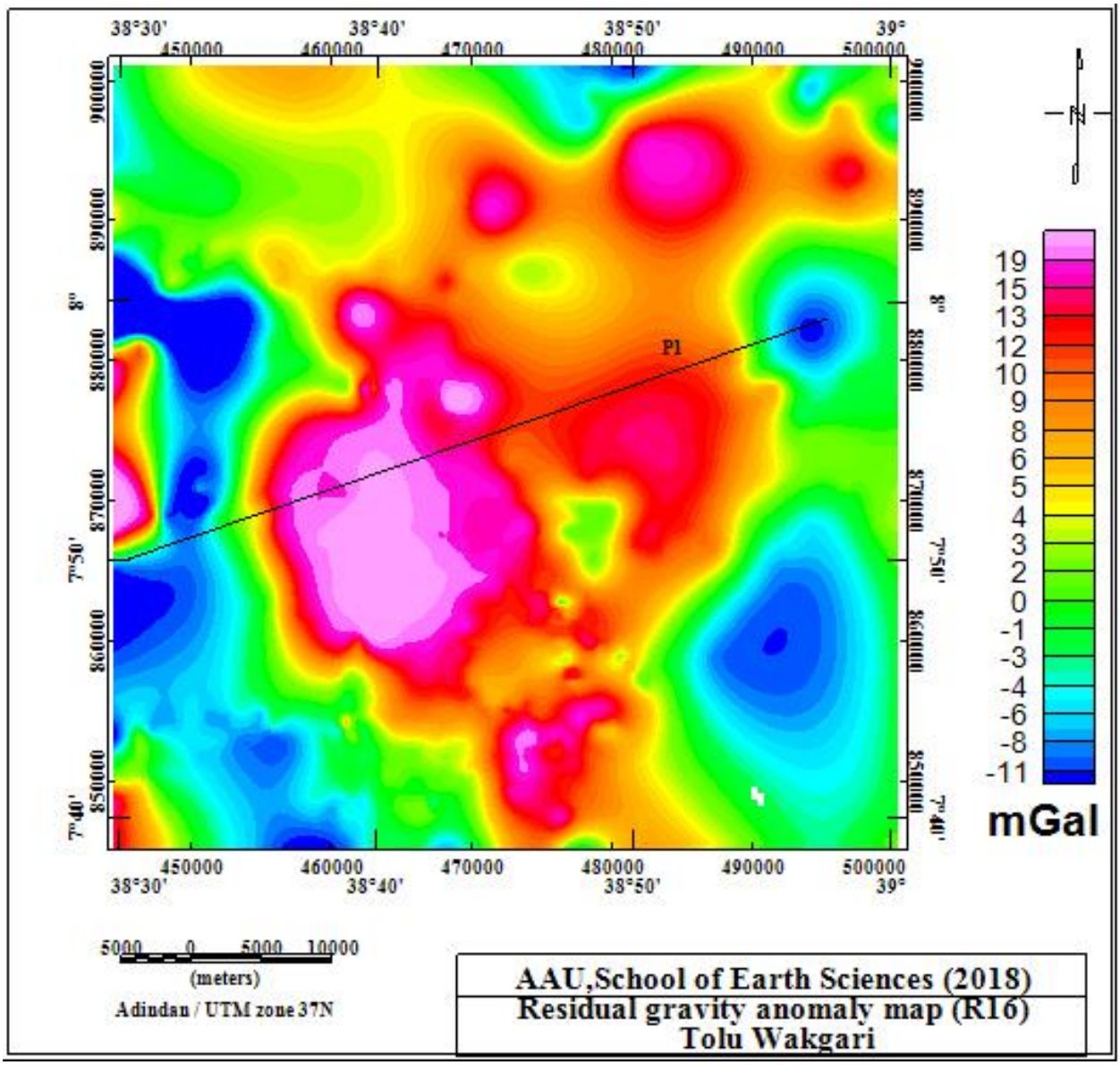

Fig. 14Residual gravity map indicating profile lines

A priori density model was obtained from the work of Saibi (2012) in the Aluo geothermal system.

Accordingly, the first layer consists of Quaternary volcanic products of Aluto volcano (ash flow tuffs, silicic lithic tuff breccias, silicic domes, pumice). The second layer consists of Pleistocene–

Holocene lacustrine sediments. The third layer includes fissural basalt, named the Pleistocene basalt. The fourth layer is represented by Tertiary ignimbrite (silicic unit).

5.4.1 2D Gravity model along profile P1

The 2D gravity model (Fig. 5.14) is constructed along profile P1 runs in an East –West (E-W) direction which is aimed to show variation in density and lithological units across the Meki-Bulbula rift corridor.

The 2D gravity model (Fig. 5.14) constructed along profile P1consists of four layers based on the depth / lithology and density constraints considered for the initial model. A further adjustment of these parameters resulted in a fit between the observed and calculated gravity values (Fig. 5.14). The error determined for the fit between the observed and calculated gravity values is 0.144 mGal.

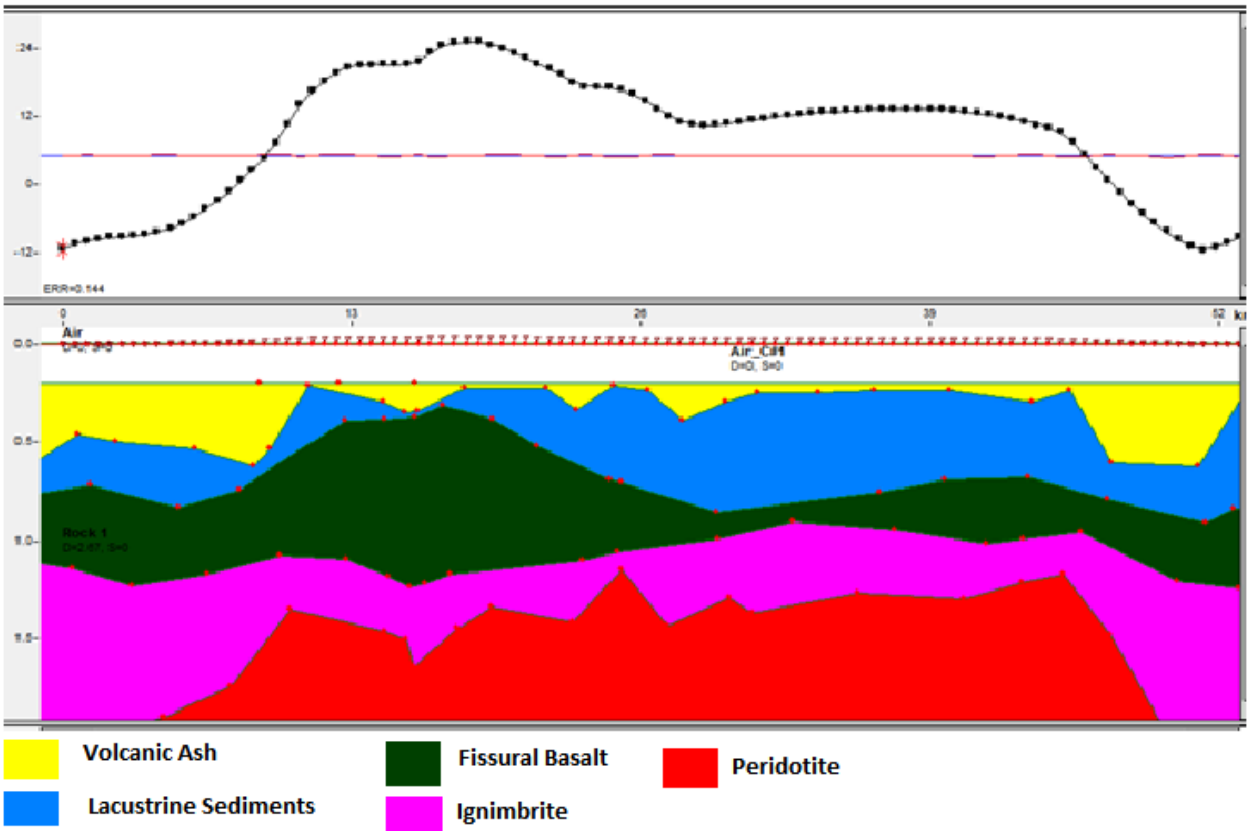

Fig. 5.15 -a2D Gravity modeling of the study area (P1)

The final gravity model corresponding to the first layer consists of relatively low density near surface volcanic ash products with an average density value of about 1700 kg/m3. The average thickness of this layer varies from 50-100 m. The second Layer has an average density value of 2180 kg/m3 with an average thickness of 150-250 m is interpreted as pleistocene – holocene lacustrine Sediments and underlain by Basalt rocks with an average thickness ranging from 300-

450m. The fourth layer is interpreted as ignimbrite rocks overlain by Basalt rocks with an average thickness ranging from 400-500m.

5.5 2D Magnetic model along profile P1

The 2D magnetic model is constructed from north western to Eastern direction using the GM-SYS modeling software to show lithologic variations along the Meki-Bulbula rift corridor. Any difference between the model response and the observed magnetic field are reduced by refining the model structure. It should be noted that magnetic models are non unique, i.e. many earth models can produce the same magnetic response, and similarly, several geological lithologies may be interpreted from a given model block's susceptibility values. It is therefore, important to use as many independent source of information as possible to constrain a model.

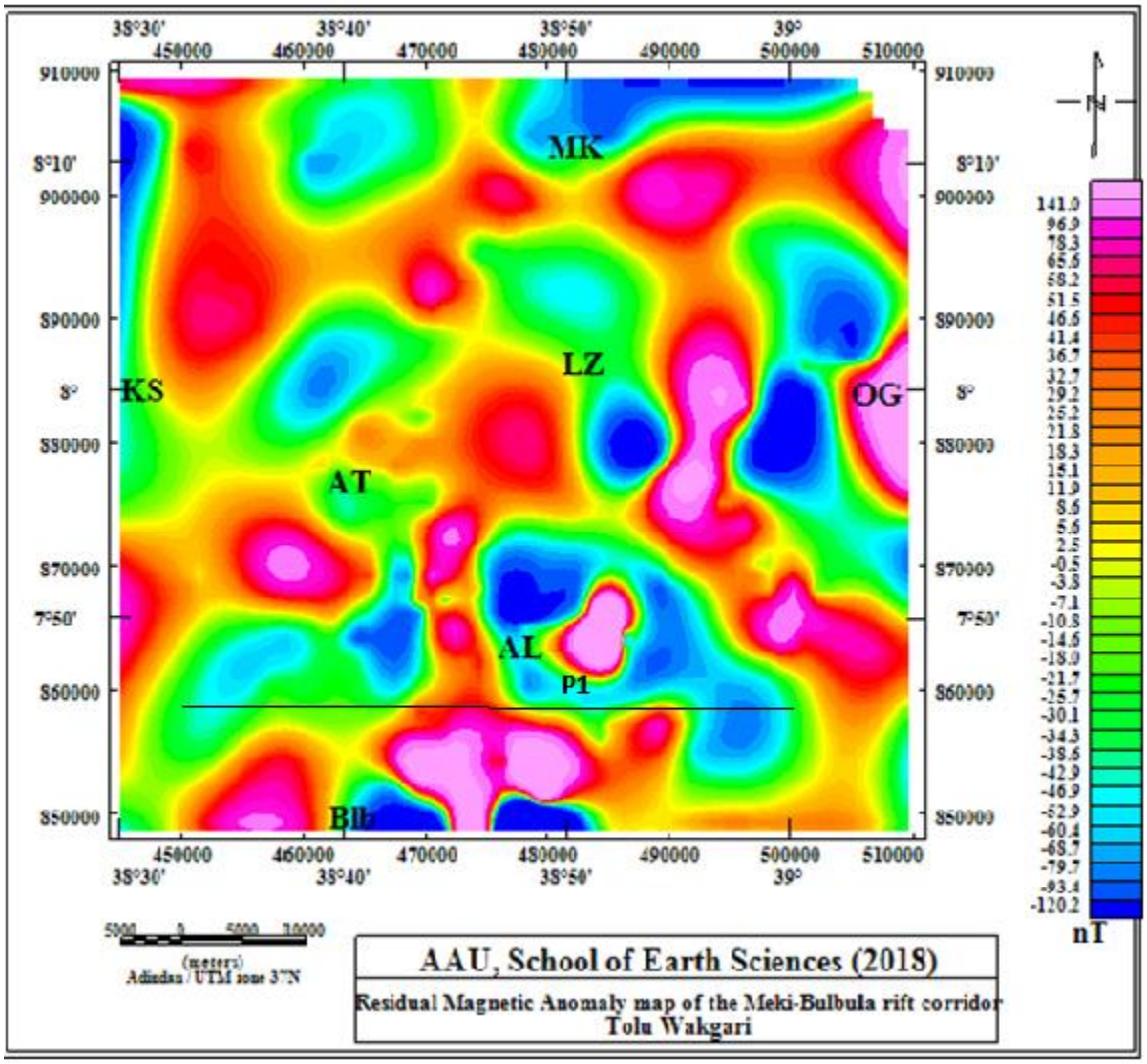

Fig. 16 Residual magnetic anomaly map of the profile line

The magnetic model corresponding to the first layer consists of relatively low sucessptibility near surface volcanic ash products with an average successptibility value of about 0.0012cgs.

The average thickness of this layer varies from 50-75 m. The second Layer has an average Magnetic susceptibility value of 0.0186 is interpreted as pleistocine – holocine lacustrine sediment with an average thickness ranges from 150-200 m and underlain by Basalt rocks with an average thickness ranging from 250-350m. The third layer shows thick fissural Basalt at the east of Lake Ziway and thin Basaltic island deposit in the Ziway Lake. The fourth layer is interpreted as ignimbrite rocks overlain by Basalt rocks with an average thickness ranging from 500-650 m. Accordingly, 2D magnetic modeling is developed along profile-1 from the residual magnetic map as shown in Figure 5.14. The developed model has an error of 0.614 nT.

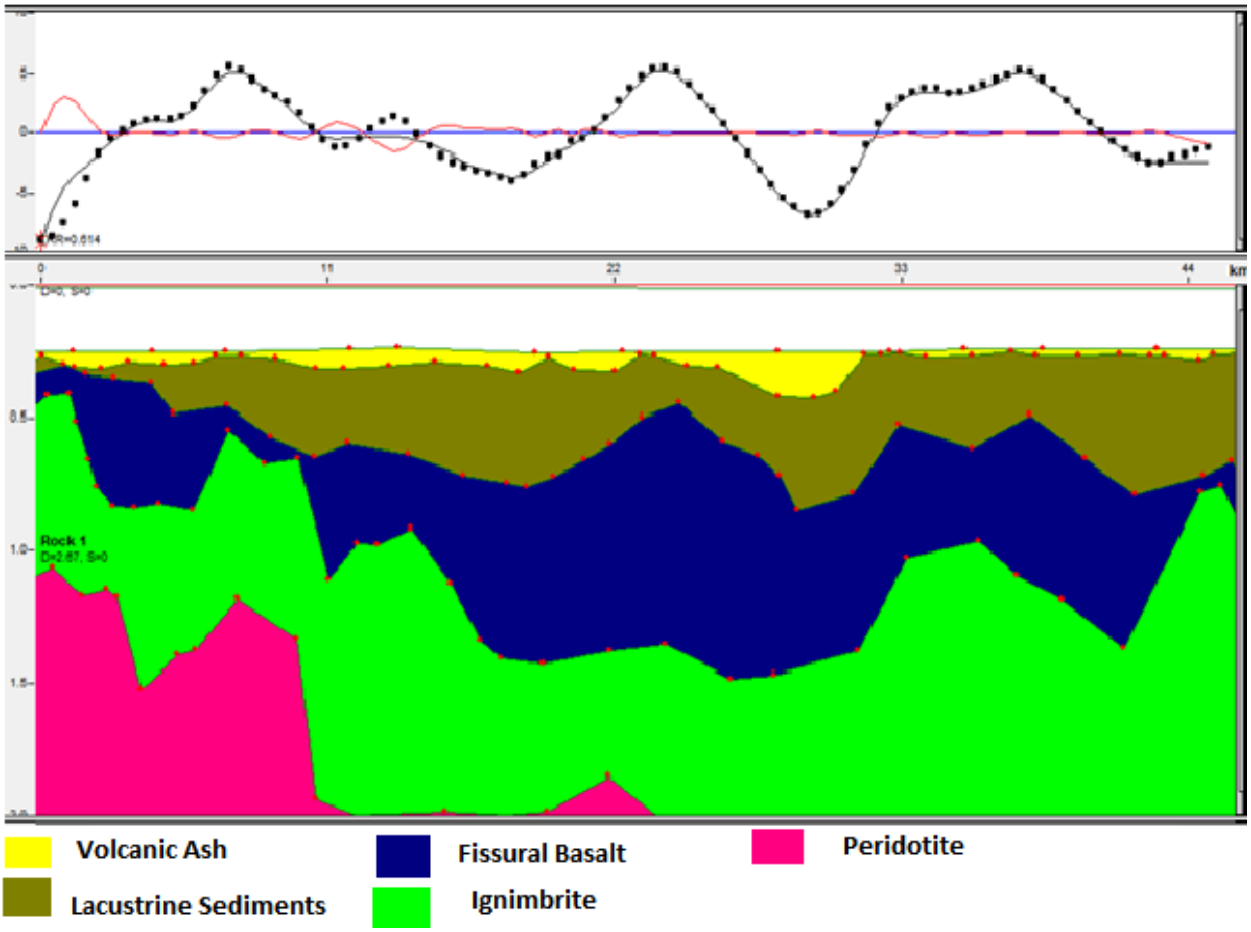

Fig. 17 2D Magnetic modeling of the study area

CHAPTER SIX

6 CONCLUSIONS AND RECOMMENDATIONS

6.1 Conclusions

Depending upon the investigations made in this study the following conclusions and recommendations are forwarded.

-The interpretation of new magnetic data with the combination of existing gravity data give us insight to constrain the nature of the subsurface structure and density distribution within the crust of the CMER and the two adjacent plateaus.

-Based the investigation results the intensity of gravity and magnetic fields are closely associated with the main structural features.

-Considering the magnetic and Gravity areas of low magnetic and Gravity anomaly (with surface manifestations and alterations) are mapped. These areas of low geophysical anomalies are interpreted to be highly water saturated region due to the close proximity of the observed profiles to the Langano and Ziway lakes.

-Lowering of density and magnetic susceptibility could imply the ground water distribution through these subsurface linear structures, which results in ground water flow.

-The N-S and NE -SW trending linear subsurface structural features revealed by both the horizontal gradient gravity map and tilt derivative Magnetic map are considered to be the major

geologic structures that favor the flow of ground water from Lake Ziway towards low lying Lake Langano.

-Depth modeled profiles comparatively show a huge deposit of fissural basalts at the southern part of the area which can help as a conduit for ground water flow as compared to other rocks.

6.2 Recommendations

Based on the outcome of this study, the following are recommended

- Additional resistivity, seismic, structural and magnetic survey data is recommended

in order to study the detailed structural geological investigations and for mapping the orientation of lineaments,

- Integrating all the geophysical results to hydro geological, geological and structural geology of the study area is important for a detailed investigation of the subsurface structures and groundwater flow of the area.

References

Abera, A. (1983). Crustal Modeling from gravity data in the Ethiopian Rift. MSc Thesis. Addis Ababa University, Addis Ababa, Ethiopia.

Abera, A. (1992). The Gravity Field and Crustal Structure of the Main Ethiopian Rift. Report **No. 26**. TRITA GEOD 1026. Stockholm, Sweden.

Abiyu, K. (2007). Groundwater flow system and hydrochemistry of ziway-koka corridor in the Main Ethiopian Rift. MSc Thesis. Addis Ababa University, Addis Ababa, Ethiopia.

Alemu, D. (2006). Groundwater–surface water interaction and analysis of recent changes in hydrologic environment of Lake Ziway catchment.

Benvenuti, M., Carnicelli, S., Belluomini, G., Dainelli, N., Di Grazia, S.,Ferrari,G.A., Iasio, C., Sagri, M., Ventra, D., Atnafu B. (2002). The Ziway–Shala lake basin (main Ethiopian rift, Ethiopia): a revision of basin evolution with special reference to the Late Quaternary.

Boccaletti, M., Mazzuoli, R., Bonini, M., Trua, T., and Bekele Abebe (1999). Plio-Quaternary volcanotectonic activity in the northern sector of the Main Ethiopian rift: Relationships with oblique rifting. *Journal of African Earth Sciences*, **29**: 679–698.

Bonini, M., Corti, G., Innocenti, F., Manetti, P., Mazzarini, F., Tsegaye Abebe, Pecskay, Z. (2005). Evolution of the Main Ethiopian Rift in the frame of Afar and Kenya rifts propagation. *Tectonics 24, TC1007*.

Corti, G. (2009). Continental rift evolution: from rift initiation to incipient break-up in the Main Ethiopian Rift, East Africa. *Earth Science Reviews.* **96:** 1 – 53.

Davidson, A. and Rex, D.C. (1980). Age of volcanism and rifting in Southwestern Ethiopia. Nature. **283**:657 – 658.

Dentith, M. and Mudge, S.T. (2014). Geophysics for the Mineral exploration Geoscientist. Cambridge University Press, New York, USA.

Dobrin, M.B. and Savit, C.H. (1988). Introduction to Geophysical Prospecting. McGraw. Hill Inc.Singapore.

GETECH Group plc. (2007). Advanced processing and Interpretation of gravity and magnetic data. Accessed on April 20, 2015 from www.getech.com.

Giday Woldegabriel, Aronson, J. L. and Walter, R. C. (1990). Geology, geochronology, and rift basin development in the central sector of the main Ethiopia rift. *Geological Society of America Bulletin*, **102(4)**: 439-458.

Hayward, N.J., Ebinger, C.J. (1996). Variations in the along-axis segmentation of the Afar Rift system. *Tectonics*, **15**: 244–257.

Hinze, W.J., VonFrese, R.B. and Saad, A.H. (2013). Gravity and Magnetic Exploration: Principles, Practices, and Applications. Cambridge University Press, New York, USA.

Kearey, P., Brooks, M. and Hill, I. (2002). An introduction to Geophysical Exploration. Third edition. *Black Well Science Ltd*, Oxford, UK.

Le Turdu, C., Tiercelin, J., Gibert, E., Travi, Y., Lezzar, K., Richert, J., Massault, M., Gasse, F., Bonnefille ,R., Decobert, M., Gensous, B., Jeudy, V., Tamrat, E., Umer, M., Koen , Martens, K., Atnafu, B., Chernet, T., Williamson, D., Taieb, M. (1999). The Ziway–Shala lake basin system, Main Ethiopian Rift: Influence of volcanism, tectonics, and climatic forcing on basin formation and sedimentation. *Palaeogeography, Palaeoclimatology, Palaeoecology*, **150**: 135–177.

Lillie, R. J. (1999). Whole Earth Geophysics: An Introduction text to geologists and geophysicists. Prentice-Hall, Inc. Upper Saddle River, New Jersey, USA

Lowrie, W. (2007). Fundamental of Geophysics. Second edition. Cambridge University Press, New York, USA.

Mesfin, T. (2017). .Applications of integrated geophysical techniques to map subsurface structures, contributing to ground water flow in the ziway – langano corridor, central main ethiopian rift. MSc Thesis. Addis Ababa University, Addis Ababa, Ethiopia.

Milsom, J. and Eriksen, A. (2011). Field Geophysics. Fourth edition. John Wiley and Sons Ltd. West Sussex, UK.

Mohr, P. (1962). The Ethiopian Rift System. *Bulletin of the Geophysical Observatory of Addis Ababa*. **5**: 33–62.

Reid, A.B., J.M. Allsop, H. Granser, A.J. Millett, and I.W. Somerton (1990). Magnetic interpretation in three dimensions using Euler deconvolution.

Mussett, A.E and Khan, M.A (2000). Looking in to the Earth: An introduction to Geological Geophysics. Cambridge University Press, USA.

Reynolds, J.M. (1997). An Introduction to Applied and Environmental Geophysics. John Wiley and Sons limited, England, UK, 415-522 pp.

Searl, R. and Gouin, P. (1972). A gravity Survey of the central part of Ethiopian Rift. In:R.W.Girdler (Editor), East African Rifts.

Saibi, H.; Aboud, E, and Ehara, S. (2012). Analysis and Interpretation of Gravity Data from the Aluto-Langano Geothermal Field of Ethiopia.

Searl, R. and Gouin, P. (1972). A gravity Survey of the central part of the Ethiopian Rift Valley. East African Rifts.

Telford, W.M., Geldart, L.P. and Sheriff, R.E. (1990). Applied Geophysics. Second edition.

Cambridge University Press. New York, USA.

Tenalem, A. (2001).Numerical Groundwater flow modeling of the Central Main Ethiopian Rift Lakes Basin. SINET: *Ethiop. J. Sci*.**24(2):**167–184.

Tsegay, B. (2015). Integrated geophysical investigations at the Corbetti-Shala-Aluto segment of the Main Ethiopian Rift: Implications for crustal structure, resources and volcanic hazards. MSc Thesis. Addis Ababa University, Addis Ababa, Ethiopia.

WoldeGabriel, G. (1987). Volcano tectonic History of the Central Sector of the Main Ethiopian Rift: a Geochronological, Geochemical, and Petrological Approach. Ph.D. Thesis

Yemane, K. (2016). Integrated geophysical investigations of the central Main Ethiopian Rift and adjacent plateaus: An implication to crustal structure and moho depth determinations. MSc Thesis. Addis Ababa University, Addis Ababa, Ethiopia.

Appendices

Appendix A: Magnetic susceptibility of common rocks

Rock type	Susceptibility emu	
	Range	Average
Igneous rocks		
Granite	0-4000	200
Ryolite	70-3000	200
Doherite	100-3000	1400
Gabbro	80-7200	6000
Basalts	70-14500	6000
Diorite	50-10000	7000
Peridotite	7600-15000	13000
Sedimentary rocks		
Dolomite	0-75	10
Limestones	2-280	25
Sandstones	0-1660	30
Shales	5-1480	50
Metamorphic Rocks		
Amphibolites		60
Phylite		130
Gneiss		130
Quartzite		350

Appendix B: Density of some common rocks

Rock type	Density	
	Range (g/cm^3)	Average (g/cm^3)
Sediments and Sedimentary rocks		
Alluvium	1.96-2.0	1.98
Silt	1.8-2.20	1.93
Soils	1.61-2.76	1.92
Sandstones	1.93-2.90	2.35
Limestone	2.28-2.90	2.55
Dolomite	2.28-2.90	2.70
Igneous rocks		
Ryolite	2.35-2.70	2.52
Dacite	2.35-2.80	2.58
Trachyte	2.42-2.80	2.60
Granite	2.50-2.81	2.64
Granodiorite	2.67-2.79	2.73
Diorite	2.70-2.99	2.85
Basalt	2.70-3.0	2.85
Peridotite	2.70-3.37	3.03
Metamorphic Rocks		
Quartzite	2.50-2.70	2.60
Phylite	2.68-2.80	2.74

Marble	2.60-2.90	2.75
Gneiss	2.59-3.0	2.80
Amphibolites	2.90-3.03	2.87